RIKEN – RESCEU joint seminar 2019
@The University of Tokyo, 20 March, 2019

Three dimensional simulation from supernovae to their supernova remnants: the dynamical and chemical evolution of SN 1987A

Masaomi ONO (RIKEN ABBL/iTHEMS)

Collaborators:

S. Orlando [2], M. Miceli [3], S. Nagataki [1], H. Umeda [4], T., Yoshida [4], T. Nozawa [5], O. Petruk [6], G. Peres [3]

1) RIKEN 2) INAF - Osservatorio Astronomico di Palermo, Italy, 3) Universita` di Palermo, Italy, 4) University of Tokyo, Japan, 5) NAOJ 6), Inst. Appl. Probl. in Mech. and Math., Ukraine

3D structure of Cassiopeia A supernova remnant

Delaney et al. 2010

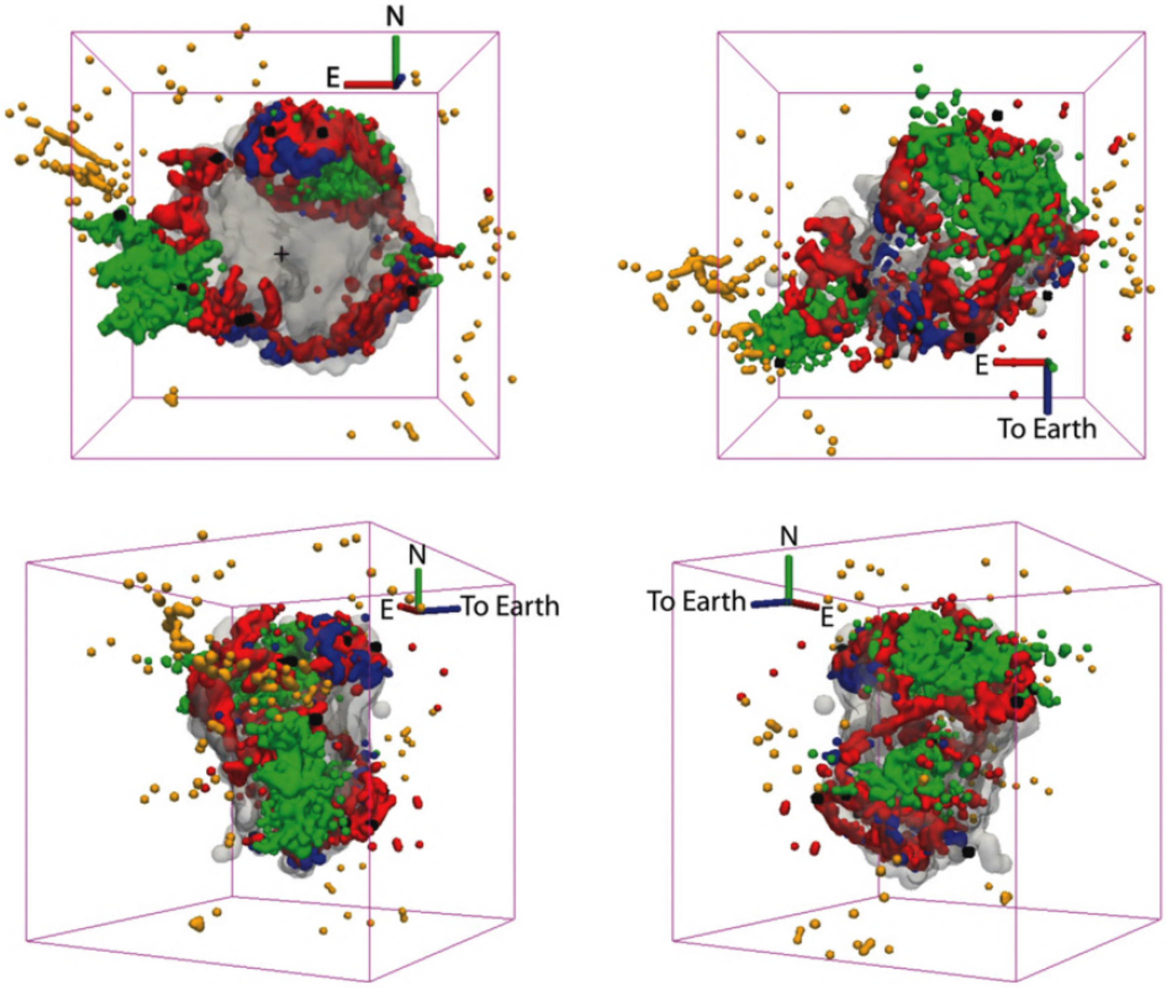

Chandra 's X-rays

Spitzer 's infrared

Green: X-ray Fe-K

Black: X-ray Si XIII

Red: IR [Ar II]

Blue: high [Ne II]/[Ar II] ratio

Grey: IR [Si II]

Yellow: optical outer ejecta

Supernova explosions to their supernova remnants (SNRs)

Supernova explosion
$t < 1$ sec

Shock breakout
$t < 1000$ sec

supernova
$t < 1$ yr

Supernova remnant
$t \sim 500$ yr

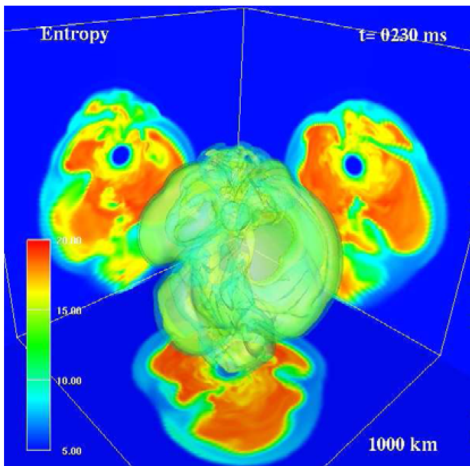

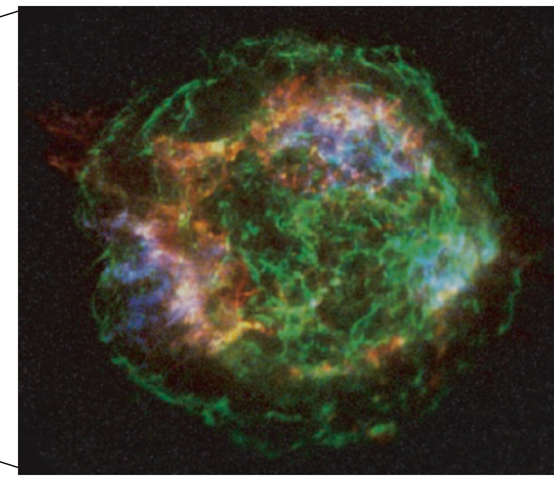

Radius of the progenitor star

$10^{7} – 10^{9}$ cm

$10^{12} – 10^{14}$ cm

$\sim 10^{18}$ cm (1 pc)

Stellar evolution of the progenitor star

Asymmetric explosion
Explosive nucleosynthesis

Matter mixing

Formation of molecules and dust?

Asymmetric distribution of elements

Chemical evolution (Nucleosynthesis/Molecule formation/dust formation) during the progenitor–SNe–SNRs sequence

NS kick velocities vs Center of Mass (CoM) velocities

Analysis of X-ray emission from six young supernova remnants

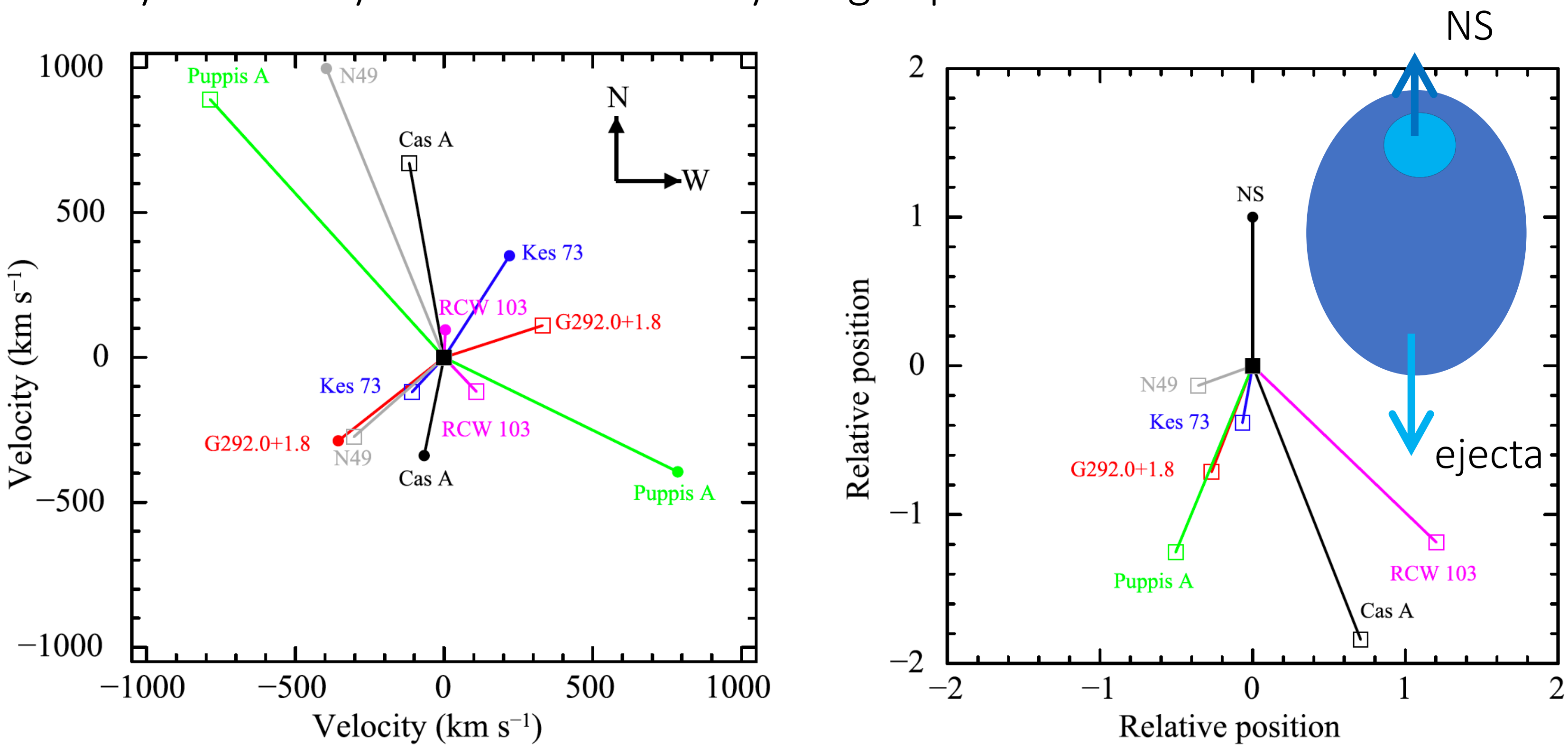

Figure 11. Left: NS kick velocities (filled circles) and the CoM velocities (open boxes) with the origin at the CoE or at the CoX for Kes 73, RCW 103, and N49, for which CoEs are not available. All opening angles between the CoM and the NS are large, which means that CoMs and NSs are located in opposite directions to the explosion points. The magnetars in Kes 73 and RCW 103 do not possess higher kick velocities than the other NSs. Right: same as the left but the NS and CoM positions are rotated such that the NS positions are aligned upward, and the velocities are normalized by the NS speeds.

Katsuda et al. 2018, ApJ, 856, 18

Supernova 1987A (SN 1987A)

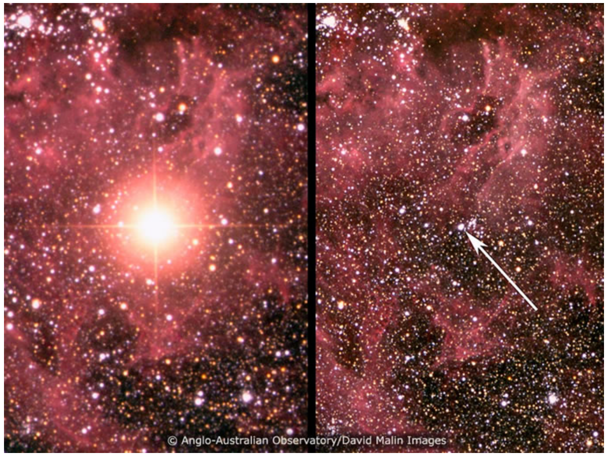

- Basic observational features of SN 1987A
  - SN @ LMC on 23 Feb., 1987
  - Neutrinos from the SN were detected by Kamiokande
  - Triple-ring nebula

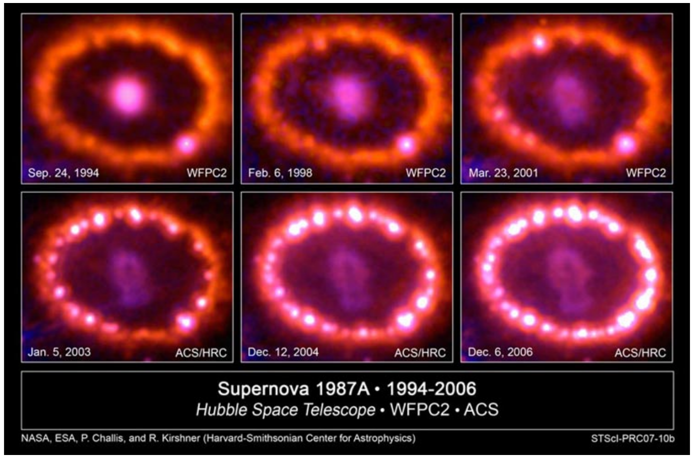

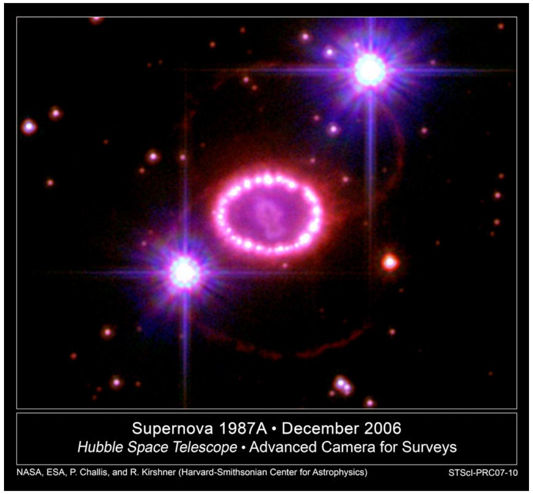

3D distribution of inner ejecta of SN 1987A

Observation from HST/STIS and VLT/SINFONI at 10,000 days after the explosion

Larsson+16, ApJ, 833, 147

Top: [Si I] + [Fe II] 1.644 μm

Bottom: H_{α}

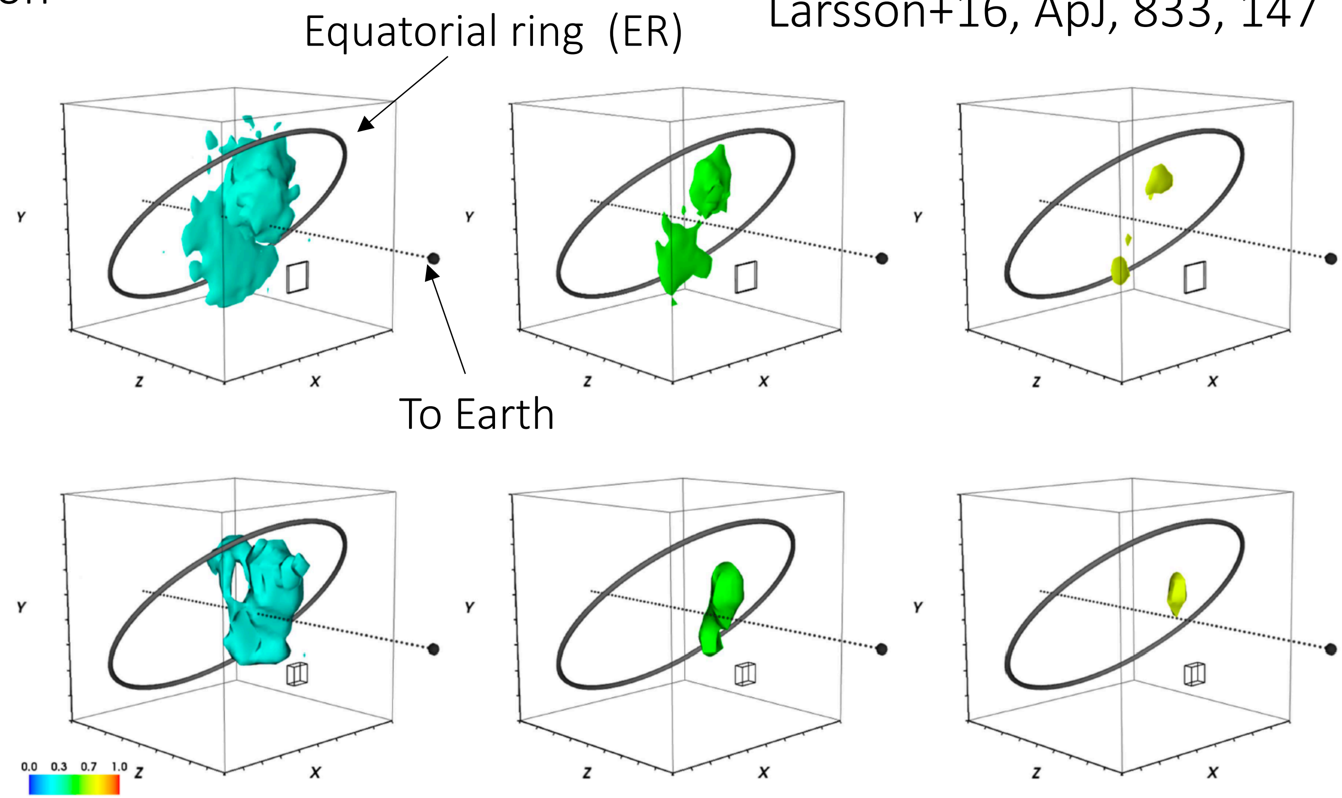

High velocity Fe : matter mixing?

[Fe II] line profiles

Haas+90', ApJ, 360, 257

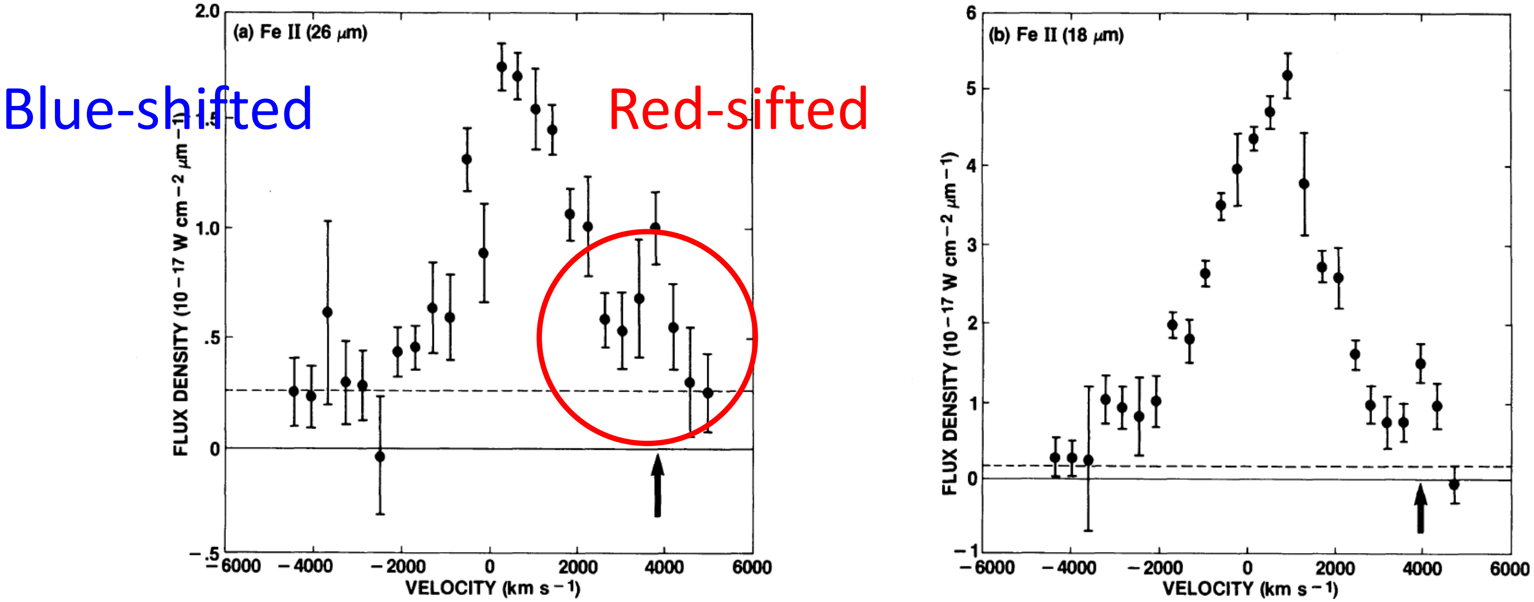

- High velocity tail of [Fe II] line profiles reach(> 4,000 km/s)

Fast ^{56}Fe (^{56}Ni -> ^{56}Co -> ^{56}Fe) motion ー＞ Matter mixing？

Red-shifted side is dominated ー＞ Asymmetric explosion?

Matter mixing in supernova explosions

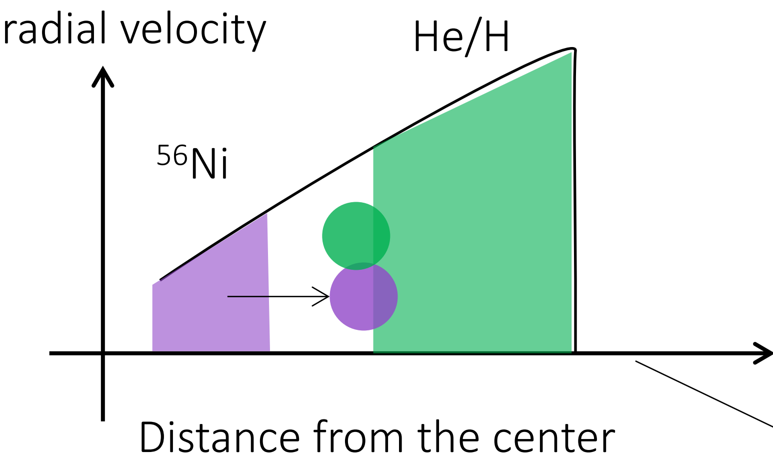

^{56}Ni is mixed up into high velocity regions ?

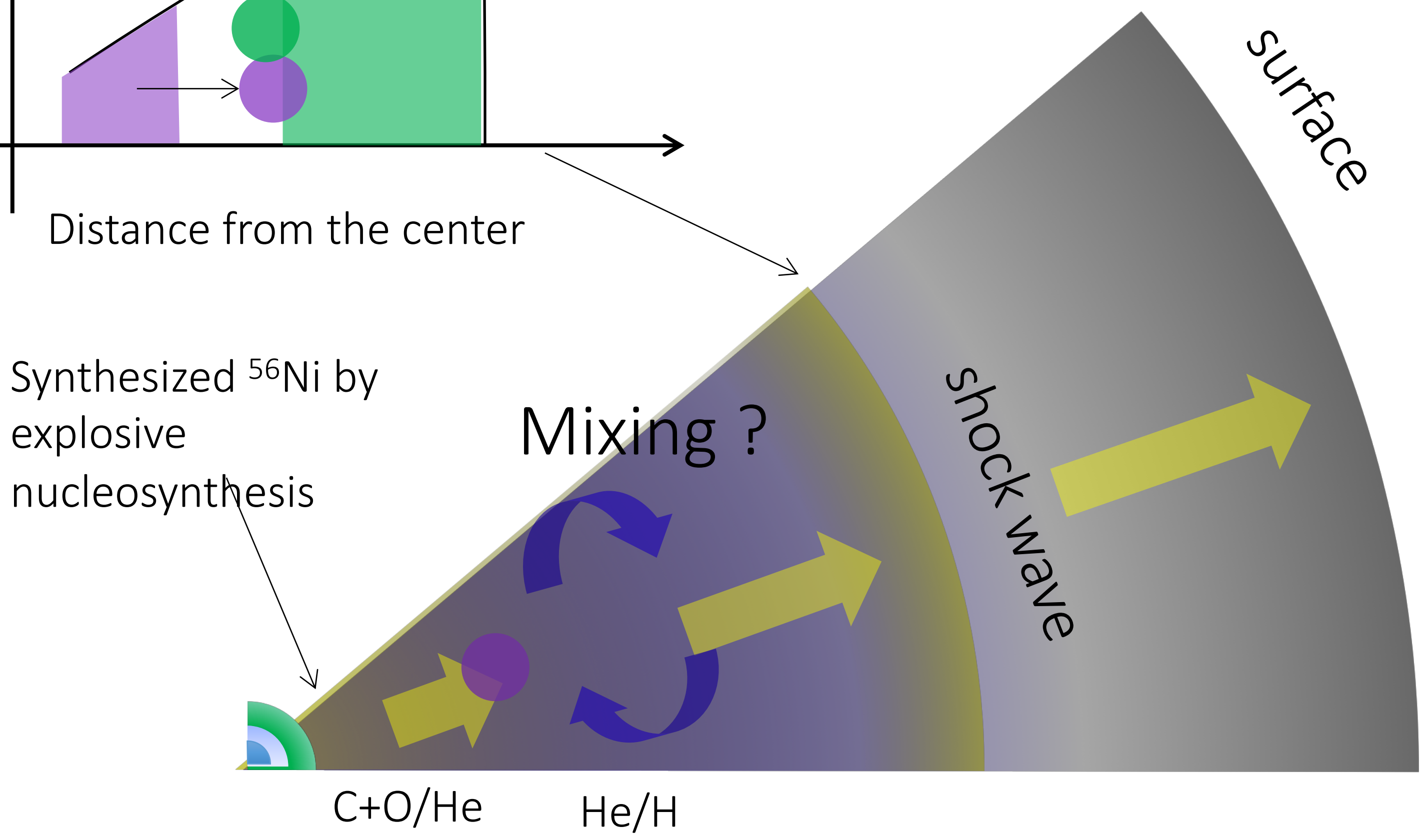

^{56}Fe (^{56}Ni -> ^{56}Co -> ^{56}Fe) が親星の外層付近まで到達 -> 物質混合か？

Rayleigh-Taylor (RT) instability

ρ_1

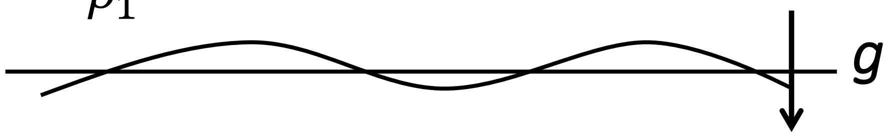

ρ_2

$\rho_1 > \rho_2$

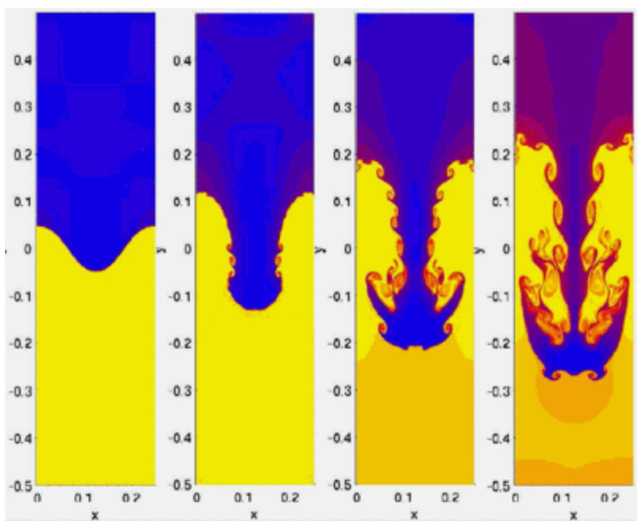

Shengtai Li & Hui Li 2006

RT unstable condition

$$\nabla \rho \cdot \nabla P < 0$$ (Chevalier 1979)

$\rho\, r^3 \searrow$ → accelerate

$\rho\, r^3 \nearrow$ → decelerate

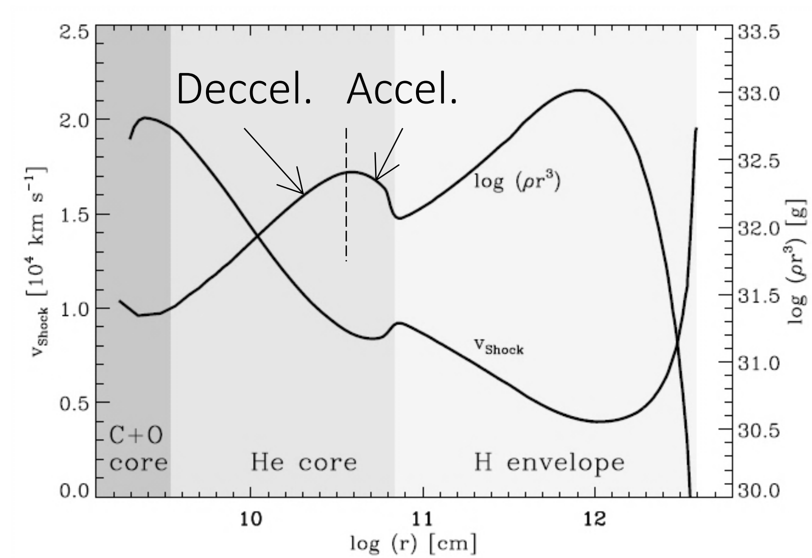

Density profile ($\rho\, r^3$) of a progenitor star

Figure is taken from Kifonidis et al. 2006

Early previous study of hydrodynamic models of the late time shock wave propagation

- 2D/3D hydrodynamic simulations
- Add hoc initiation of spherical supernova explosion
- RT mixing at O/He, He/H interfaces
- Maximum ^{56}Ni velocity around 2000 km s^{-1}

Spherical explosion + RT instability could not explain the observed high velocity of ^{56}Ni

Arnett et al. 1989; Fryxell et al. 1991, Mueller et al. 1991b,a,c; Hachisu et al. 1990, 1991, 1992, 1994; Herant & Benz 1991; Herant & Benz 1992

Simulations of non-spherical explosions

- 2D Jet like explosions (Yamada & Sato 1991; Nagataki et al. 2000)
- 2D neutrino-driven explosion
  (Kifonidis et al. 2006; Gawryszczak et al. 2010)

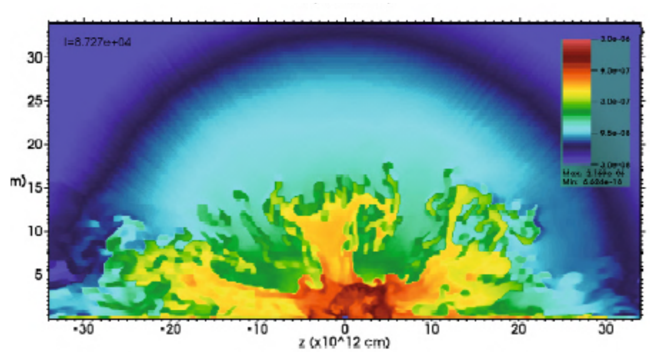

Maximum ^{56}Ni velocity obtained: about 4000 km s^{-1}

Density distribution 7 days after the explosion of SN 1987A

- 3D (Hammer et al. 2010; Wangwathanarat et al. 2015)
- SPH (Hungerford et al. 2003,2005; Ellinger et al. 2012)
- 2D (MO et al. 2013; Mao et al. 2015)

^{44}Ti gamma-ray emission lines from SN1987A reveal an asymmetric explosion

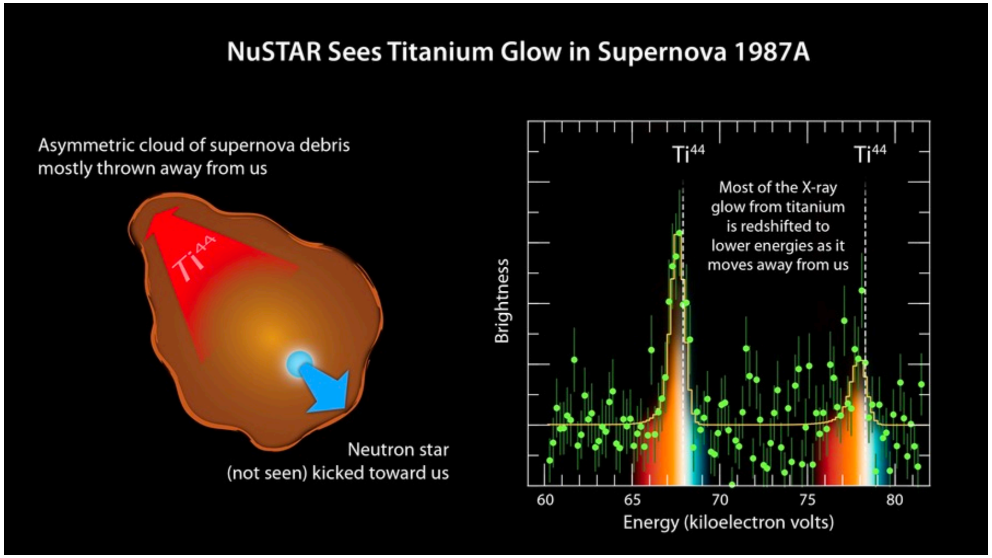

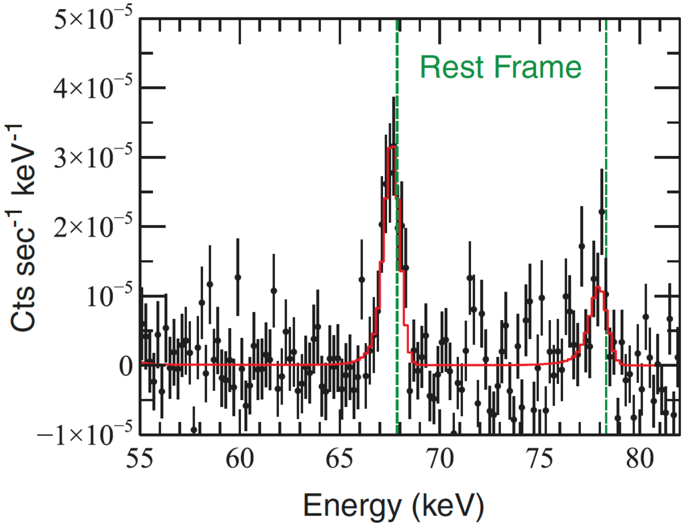

59-80 keV NuSTAR spectrum of SN1987A with detected ^{44}Ti emission lines.
[Credit: NASA/JPL-Caltech/UC Berkeley]

Figure from https://nustar.ssdc.asi.it/news.php

- Observations of ^{44}Ti lines by NuSTAR
- Lines are redshifted with a Doppler velocity of about 700 km/s
- An asymmetric explosion is invoked

Boggs et al. 2015, Science, 348, 670

Properties of the progenitor of SN 1987A

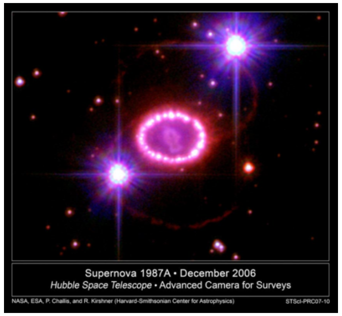

- Observational features of Sk-69° 202 at LMC
  - Blue supergiant (BSG)
  - Triple ring structure
  - log ($L/L_\odot$) = 4.89 – 5.17 & $T_{\rm eff}$ = 15 – 18 kK [Woosley 1988]
  - log ($L/L_\odot$) = 4.90 – 5.11 & $T_{\rm eff}$ = 12 – 19 kK [Barkat & Wheeler 1989]
  - Red to Blue transition at least 2 x 10^4 yr ago [Crotts & Heathcote 1991]
  - Nebula abundance:
    He/H = 0.17 ± 0.06, N/C = 5 ± 2 [Lundqvist & Fransson 1996; Mattila et al. 2010]
    N/O = 1.1 ± 0.4 [Lundqvist & Fransson 1996]
    N/O = 1.5 ± 0.7 [Mattila et al. 2010]
- Preferable conditions for the progenitor star model [Arnett 1989, ARA&A, 27, 629]
  - helium core mass: 6 ± 1 $M_\odot$
  - Radius: (3 ± 1) x 10^{12} cm
  - Hydrogen envelope mass : about 10 $M_\odot$

3D simulation of neutrino-driven explosions: progenitor dependences

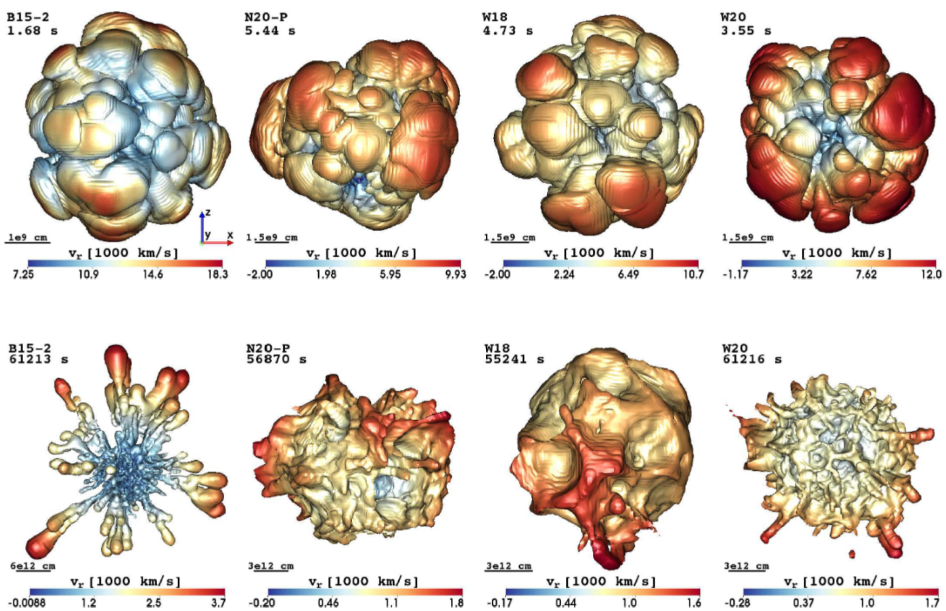

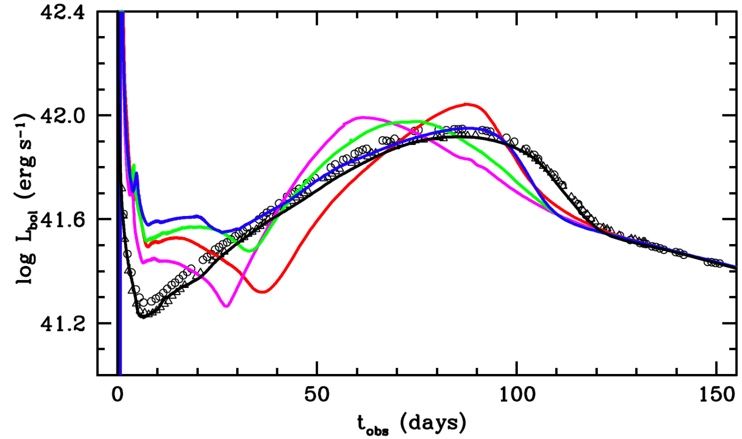

Utrobin, Wangwathanarat, Janka and Mueller 2015

Model	$\langle v\rangle^{\rm bulk}_{\rm Ni}$	$v^{\rm bulk}_{\rm Ni}$ (km s^{-1})	$\langle v\rangle^{\rm tail}_{\rm Ni}$	$M_{\rm mix}$	$\delta M_{\rm H}$ ($M_\odot$)	$\langle X\rangle$
B15-1	921	3103	3241	11.45	0.111	0.040
B15-2	1222	3355	3490	11.20	0.172	0.062
B15-3	1807	4977	5678	12.31	0.329	0.118
N20-P	924	1635	1790	4.80	0.262	0.039
N20-C	930	1642	1797	4.79	0.375	0.052
W18	877	1395	1472	4.10	0.062	0.011
W20	783	1374	1482	5.32	0.083	0.012

- B15-2 model seems to be good but...
  - He core mass (4.05 $M_\odot$) is quite different from the required value, 6 $M_\odot$
  - The synthesized the light curve

The progenitor of SN1987A was the outcome of a binary merger?

- 3D smoothed particle hydrodynamic (SPH) simulation

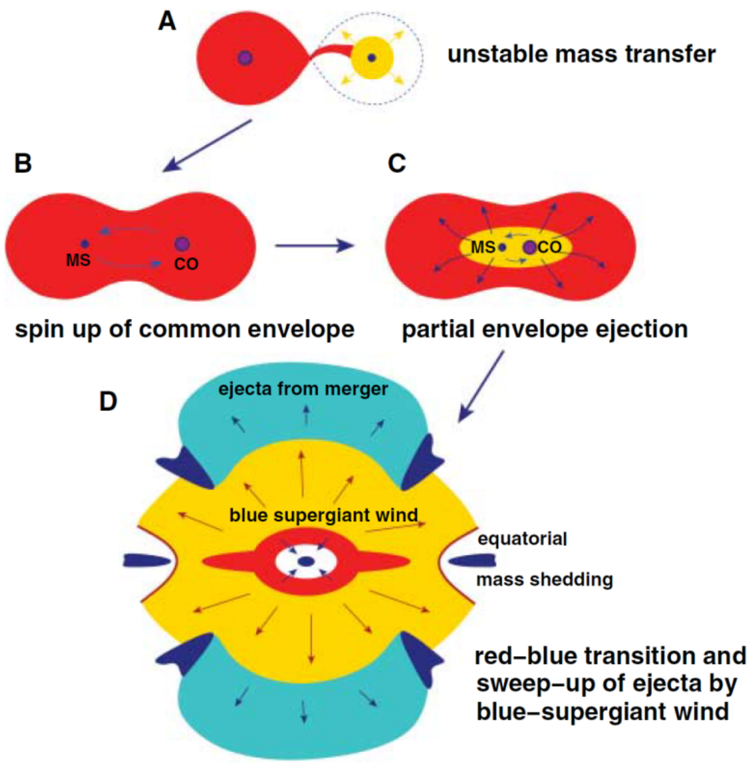

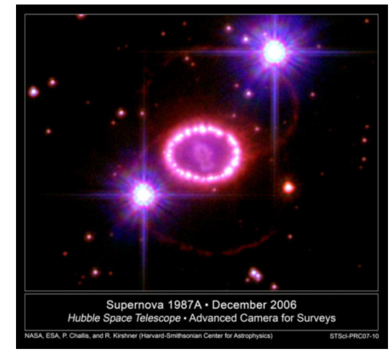

E

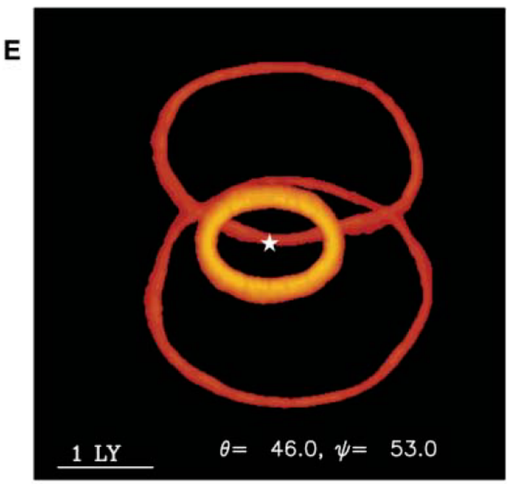

Morris & Podsiadlowsky 2007, Science, 315, 1103

Binary merger models of the Progenitor of SN 1987A

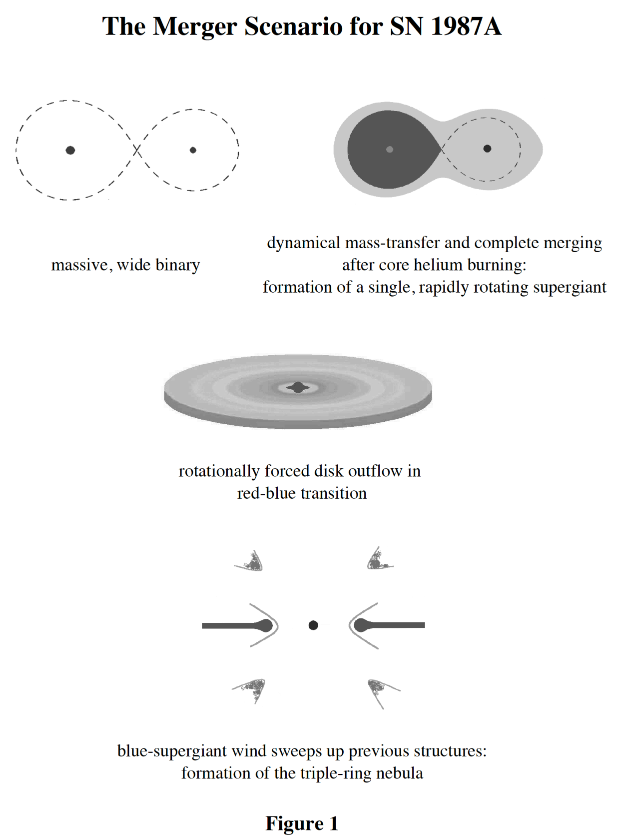

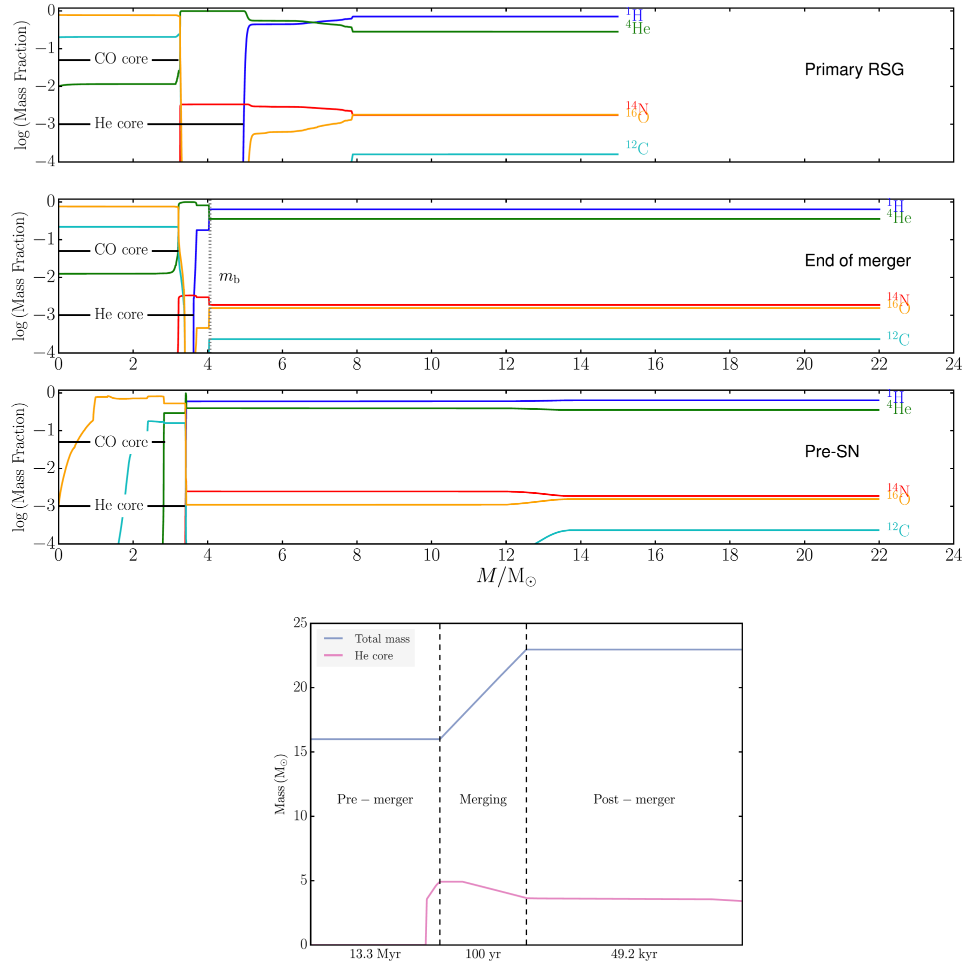

Morris & Podsiadlowsky 2007;
Podsiadlowski 2017: arXiv:1702.03973

Menon & Heger 2017, MNRAS, 469, 4649

X-ray light curves, covering late 16 years

Frank et al. 2016, ApJ, 829, 40

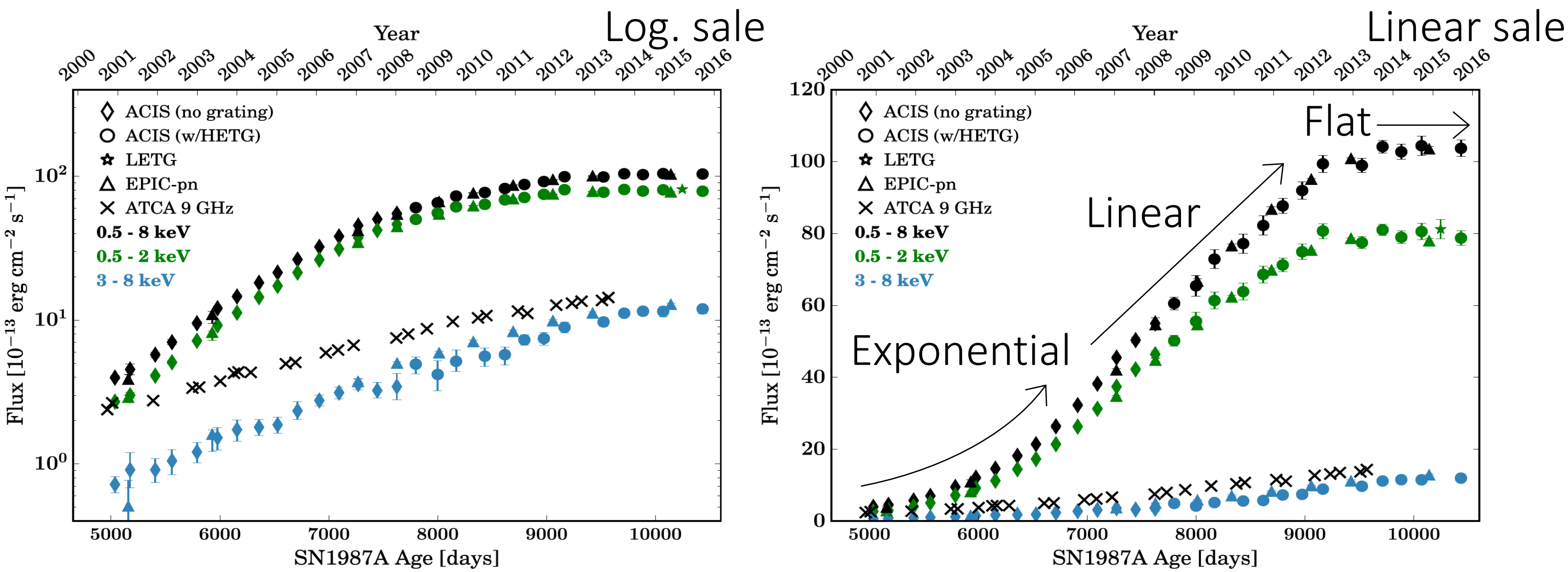

- Sharp upturn of soft components (6000 days): blast wave impacting ER
- Linear evolution (7000 - 8000 days): stop of density increase
- Nearly constant flux (9500 days): blast wave leaves the dens ER
- Hard component increases slowly: shocks moving lower density regions

X-ray images and evolution of E/W asymmetry

Frank et al. 2016, ApJ, 829, 40

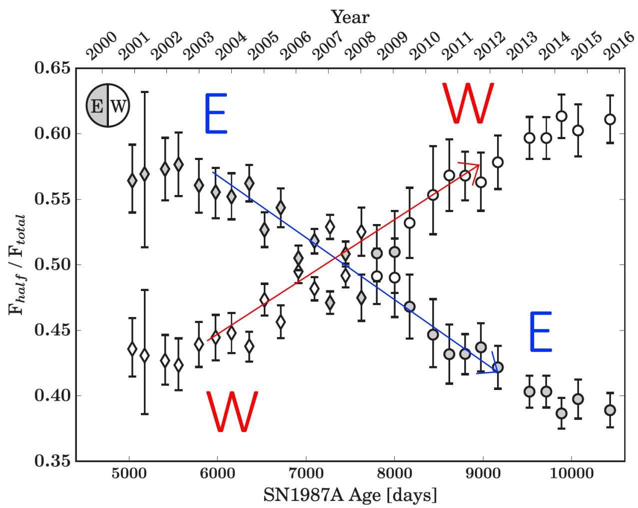

Figure 6. Fraction of the total 0.3–8 keV flux in the east (filled symbols) and west (empty symbols) halves of the ER over time. The center of the ring for each observation is defined as the center of the ring from our best-fit model as described in Section 3.3. Symbols are the same as Figure 2. The fractional fluxes of the individual southeast and northeast quadrants evolve similarly over time (both decreasing), as do the western quadrants (both increasing).

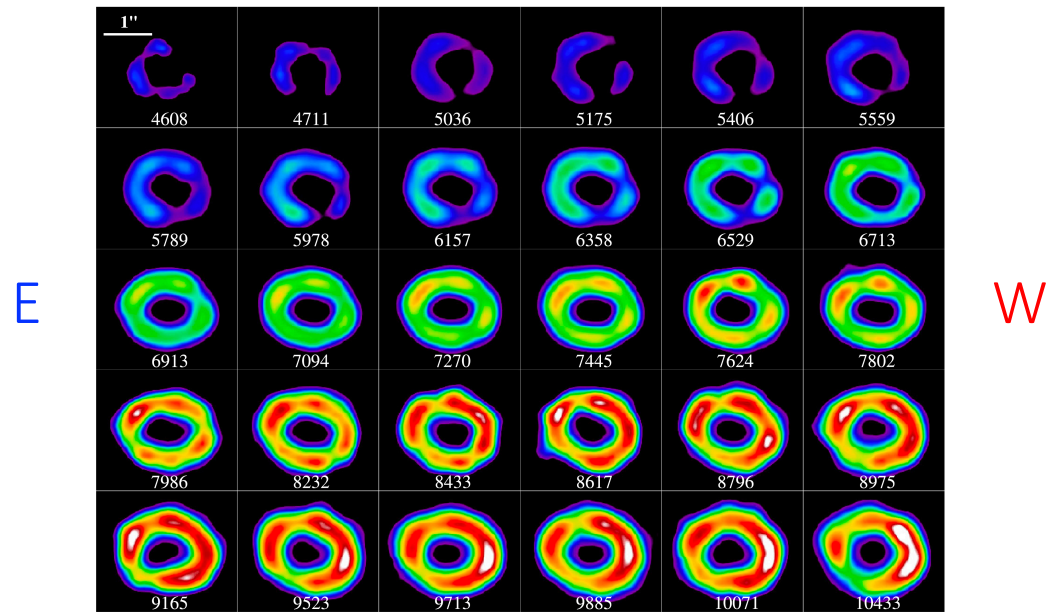

Figure 5. Deconvolved, smoothed 0.3–8.0 keV false-color images of SN 1987A covering days 4608–10433. Images use a square root scale and are normalized by flux. The age, in days since the supernova, is shown below each image. North is up and east is to the left.

- X-ray emission first appeared on the eastern side of ER
- The eastern side began to fade (7000 days)
- E/W X-ray emission reversed during 7000 – 8000 days

Molecule distribution in 3D

Abellán et al. 2017, ApJ, 842, L24

ALMA observations of CO J = 2 -1, SiO J = 5 – 4, 6 -5 rotational transitions

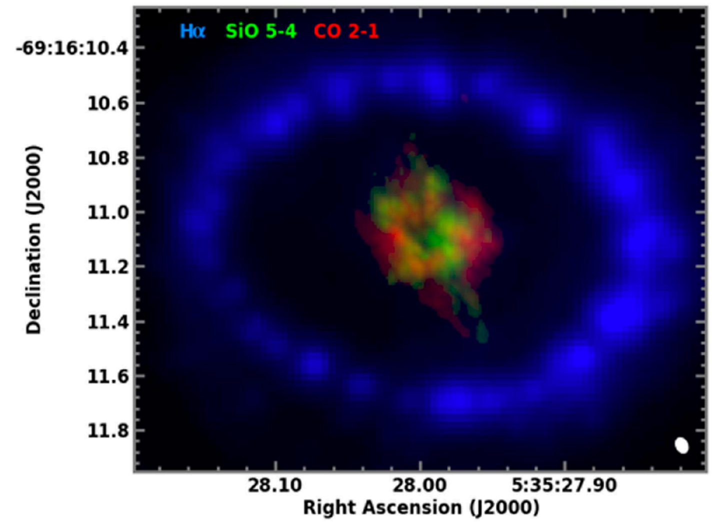

Figure 1. Molecular emission and Hα emission from SN 1987A. The more compact emission in the center of the image corresponds to the peak intensity maps of CO 2−1 (red) and SiO 5−4 (green) observed with ALMA. The surrounding Hα emission (blue) observed with *HST* shows the location of the circumstellar equatorial ring (Larsson et al. 2016).

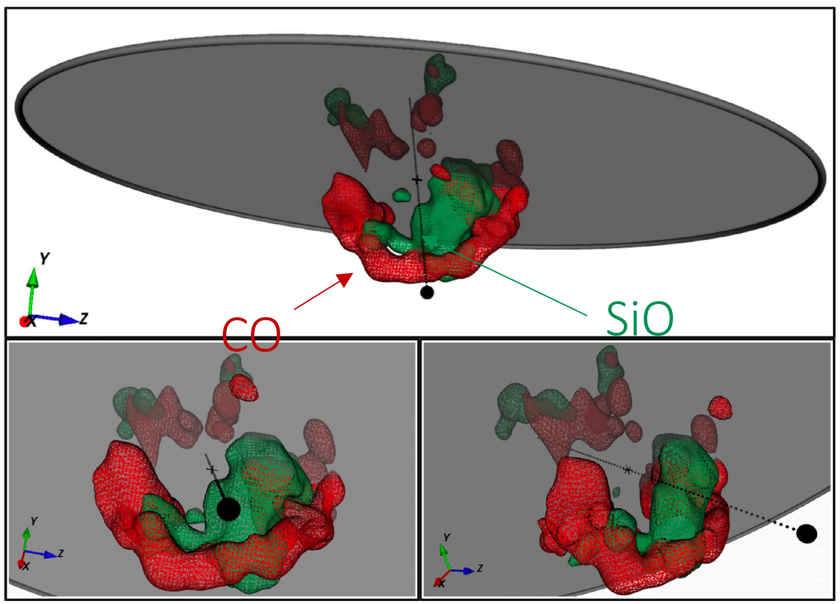

Figure 2. 3D view of cold molecular emission in SN 1987A. The CO 2−1 (red) and SiO 5−4 (green) emission is shown from selected view angles. The central region is devoid of significant line emission. The emission contours are at the 60% level of the peak of emission for both molecules. The black dotted line and black filled sphere indicate the line of sight and the position of the observer, respectively. The gray ring shows the location of the reverse shock at the inner edge of the equatorial ring (*XZ* plane). The black cross marks the geometric center.

(An animation of this figure is available.)

SN 1987A: A template to link supernovae to their remnants (Orlando+15)

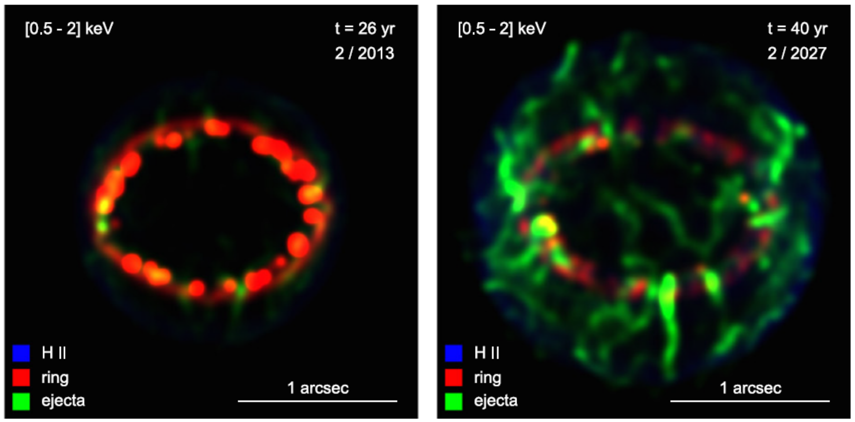

Images of X-ray emission

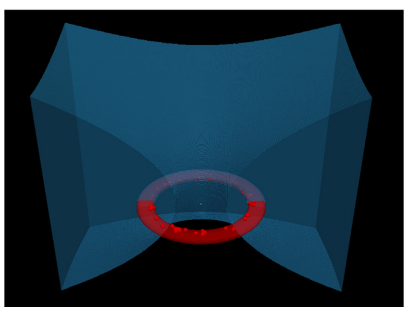

Initial distribution of the ER and HII region

Orlando et al. 2015, ApJ, 810, 168

Synthesized X-ray light curves

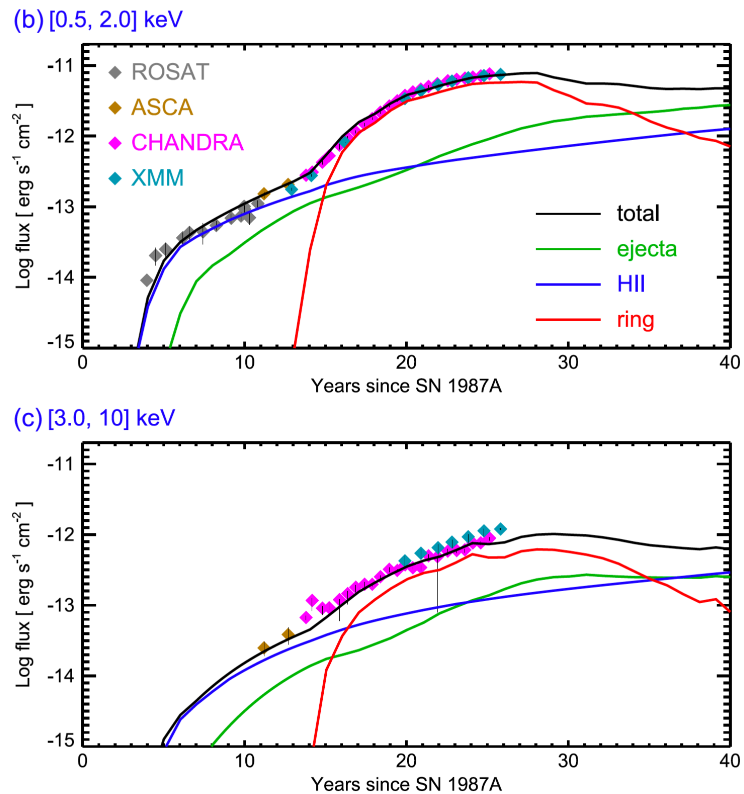

1D spherical explosion is assumed

Effect of B-field on the survival of clump structures in the ER ring

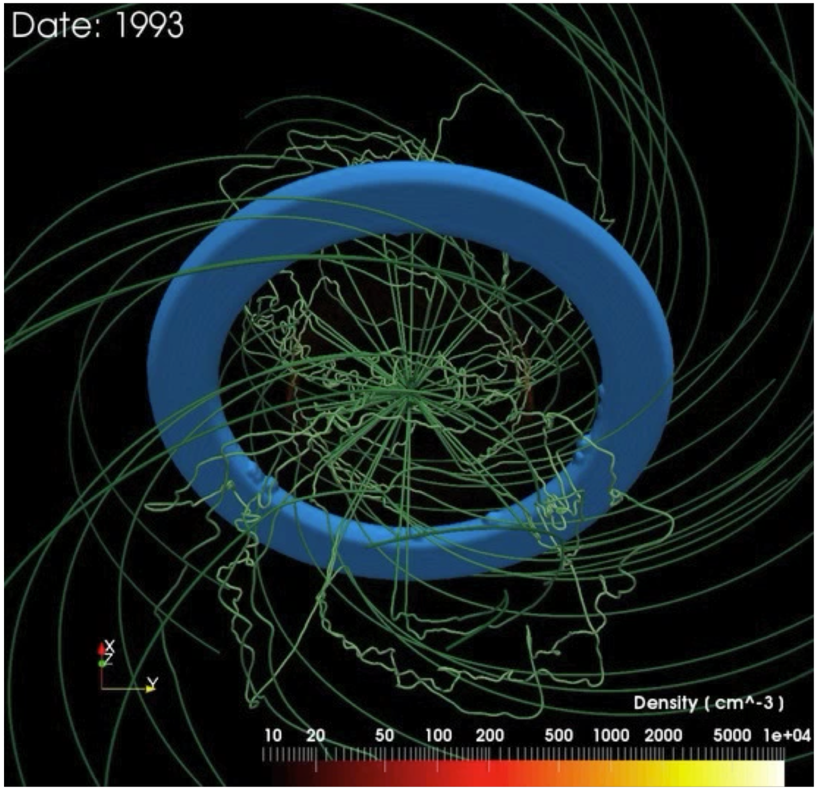

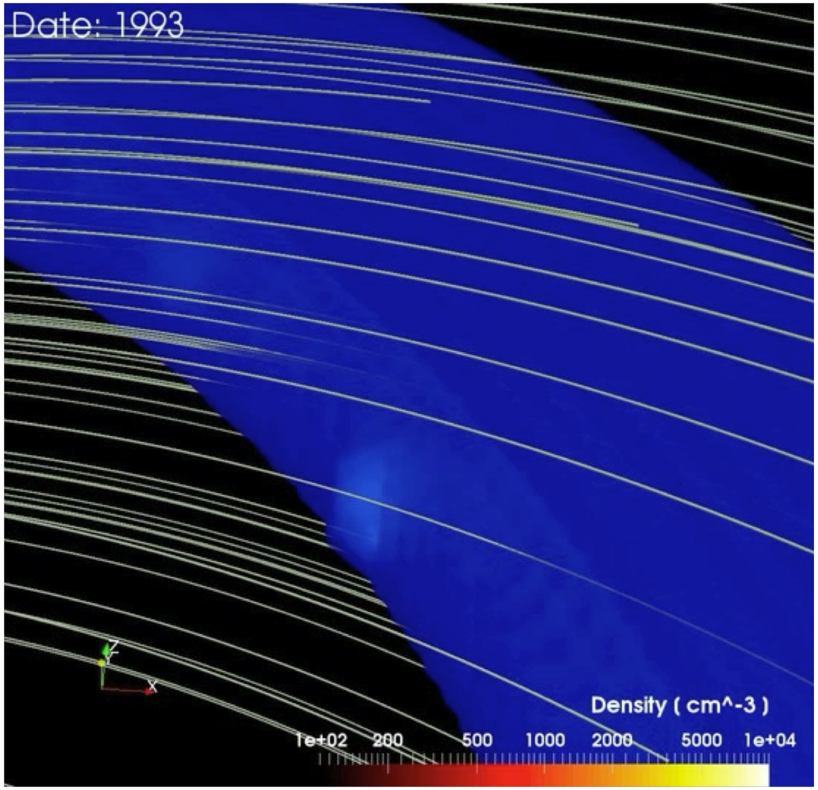

Orlando et al. 2018, A&A, 622, A73

3D simulation from Supernovae to Supernova remnants

3D simulation of SNe

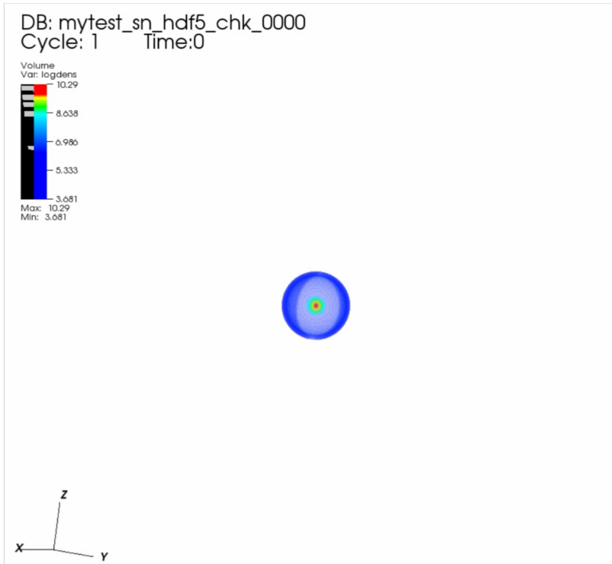

Aspherical explosion
Nucleosynthesis

1 sec,1000 km

3D MHD simulation of SNRs

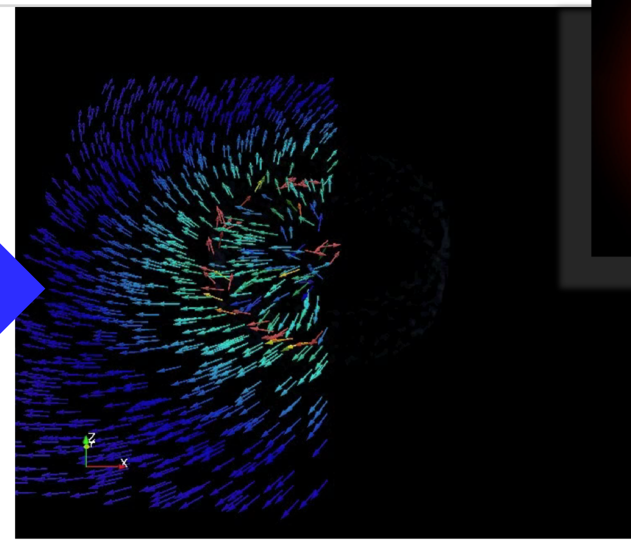

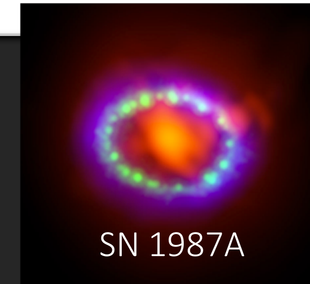

X-ray light curve, X-ray Image,
Non-thermal emission

10 – 100 yr, 10^{12} – 10^{13} km

PRACE project: Awarded and we got 6×10^{7} CPU hours at a cluster of CINECA

Masaomi Ono (ABBL, RIKEN, Japan)
Shigehiro Nagataki (ABBL, RIKEN, Japan)
Gilles Ferrand (ABBL, RIKEN, Japan)
Annop Wongwathanarat (ABBL, RIKEN, Japan)
Shiu-Hang Lee (Kyoto Univ., Japan)
Ko Nakamura (Fukuoka Univ., Japan)
Tomoya Takiwaki (NAOJ, Japan)

Salvatore Orlando (INAF – *, Italy)
Marco Miceli (**, Italy)
Oleh Petruk (INAF – *, Italy)
Giovanni Peres (**, Italy)

* Osservatorio Astronomico di Palermo
** Universita` di Palermo

Density structures of two progenitor models used

Binary merger model (purple)

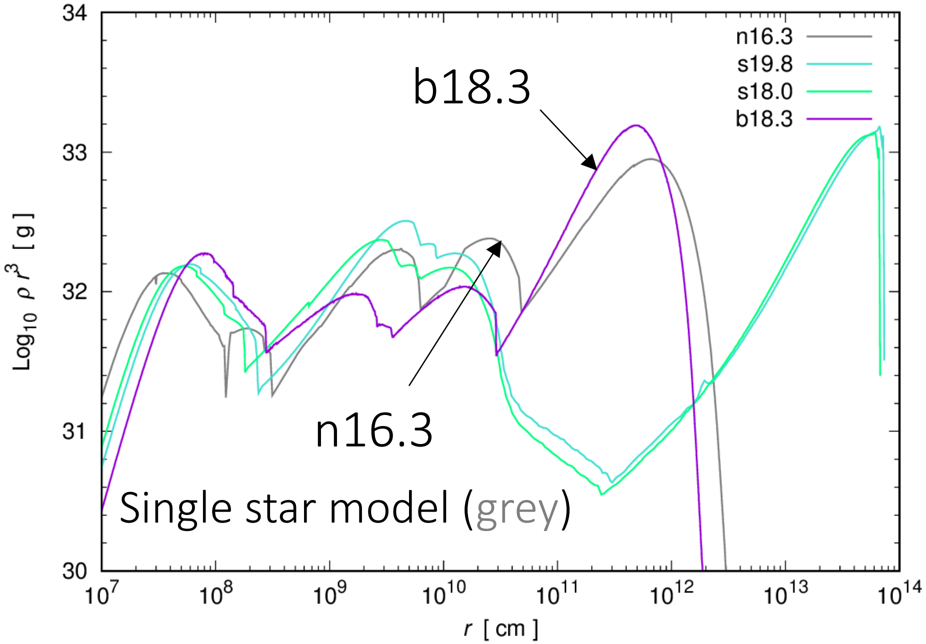

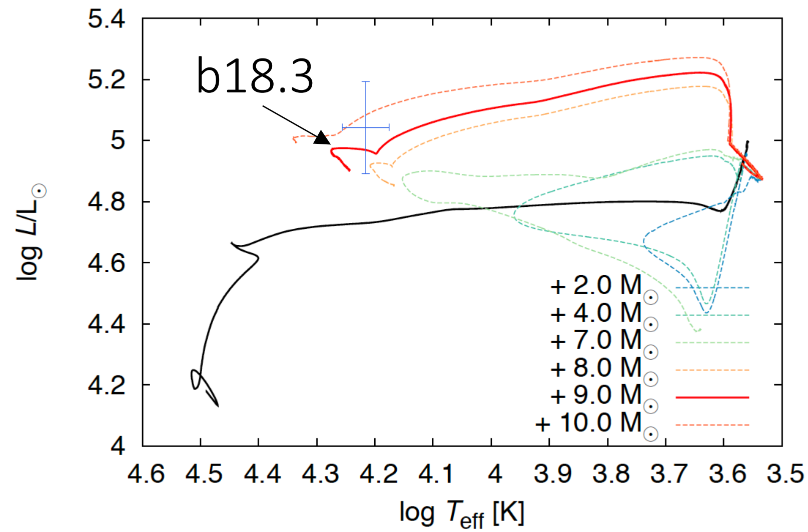

Slow binary merger scenario model

From the self-similar solution in the power law density medium

Urushibata, T., Takahashi, K., Umeda, H., & Yoshida, T. 2017, MNRAS, 473, L101

$\rho(r) \propto r^{-\omega}$ $v_{\rm sh} \propto t^{(\omega-3)/(5-\omega)}$ If $\omega < 3$ shock is decelerated

Initial setup: radial velocity distribution

Parameters

$\beta = v_{\rm pol}/v_{\rm eq}$

$\alpha = v_{\rm up}/v_{\rm down}$

$E_{\rm in}$: Injected energy

Ranges:

$E_{\rm in}$ = (1.5 – 3.0) x 10^{51} erg

β = 1.0 – 16.0

α = (1.1 – 1.5)

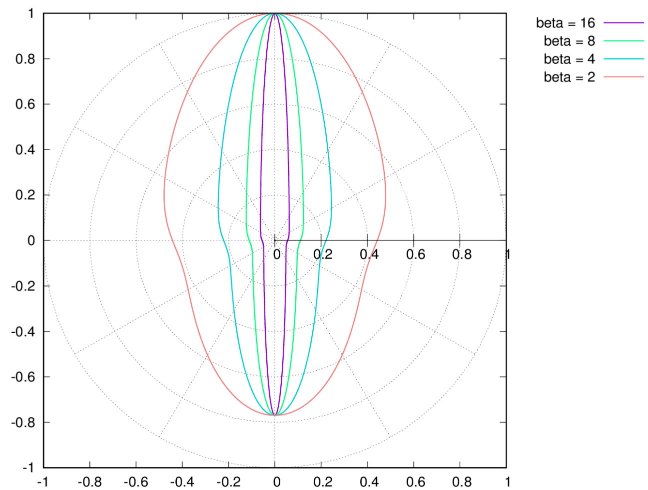

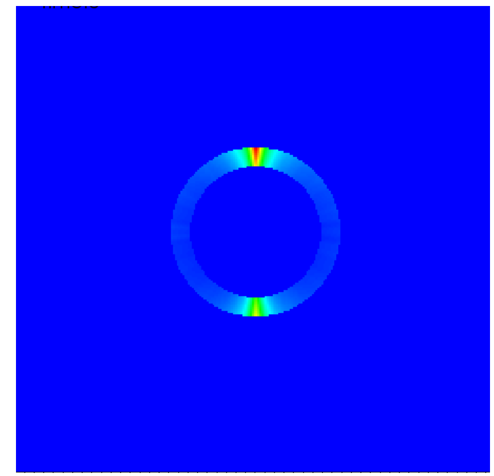

$$v_r \propto r \left(\beta^{-1}\cos^2\theta + \beta\sin^2\theta\right)^{-1/2}$$

$$1 + \epsilon N \sum_n^4 \sum_m \frac{A_m^l(\theta,\phi)}{2^{n-1}} \qquad (l = n \cdot l_{\rm base})$$

$$\epsilon = 0.3,\ l_{\rm base} = 15$$

N : Normalization factor

$$A_m^l(\theta,\phi) = \begin{cases} \begin{cases} Y_m^l(\theta,\phi) & (m = 1, -3, 5, -7, ..) \\ 0 & (\text{else}) \end{cases} & (l : \text{odd}) \\ \begin{cases} Y_m^l(\theta,\phi) & (m = 0, 2, -4, 6, ..) \\ 0 & (\text{else}) \end{cases} & (l : \text{even}) \end{cases}$$

$$Y_m^l(\theta,\phi) = \begin{cases} \sqrt{2}\sqrt{\frac{2l+1}{4\pi}\frac{(l-|m|)!}{(l+|m|)!}} P_m^l(\cos\theta)\sin(|m|\phi) & (m < 0) \\ \sqrt{\frac{2l+1}{4\pi}} P_m^l(\cos\theta) & (m = 0) \\ \sqrt{2}\sqrt{\frac{2l+1}{4\pi}\frac{(l-|m|)!}{(l+|m|)!}} P_m^l(\cos\theta)\cos(m\phi) & (m > 0) \end{cases}$$

Time evolution of 2D slices of density : binary merger model vs single star model

MO et al. 2019a, in prep.

b18.3 movie n16.3

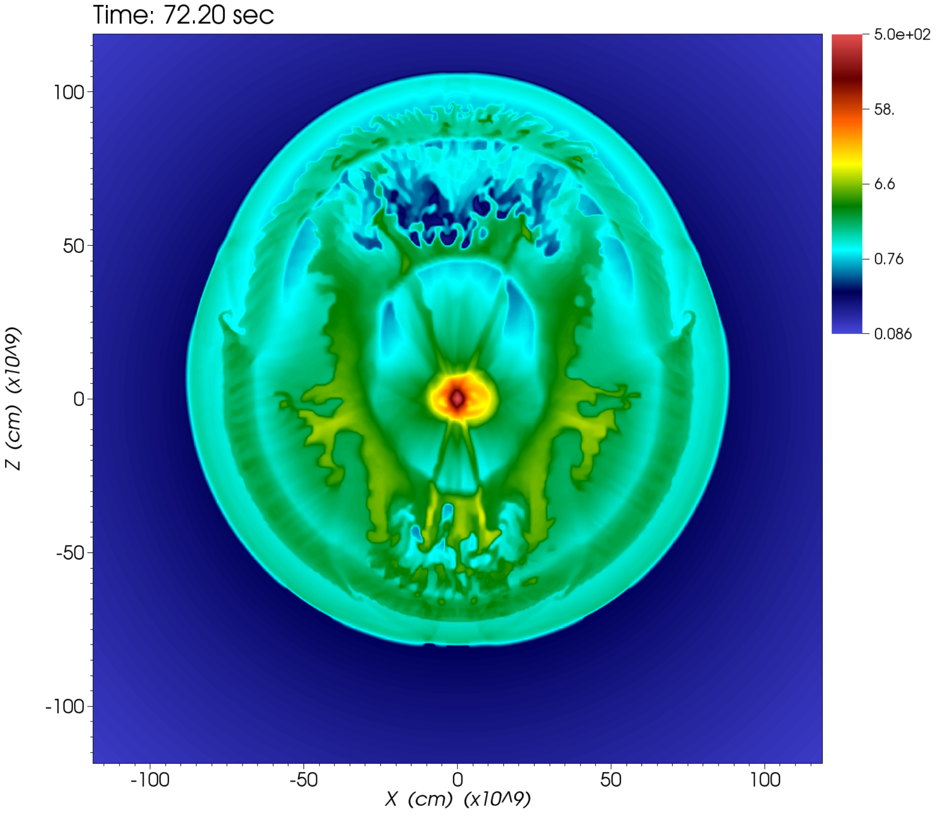

Binary merger

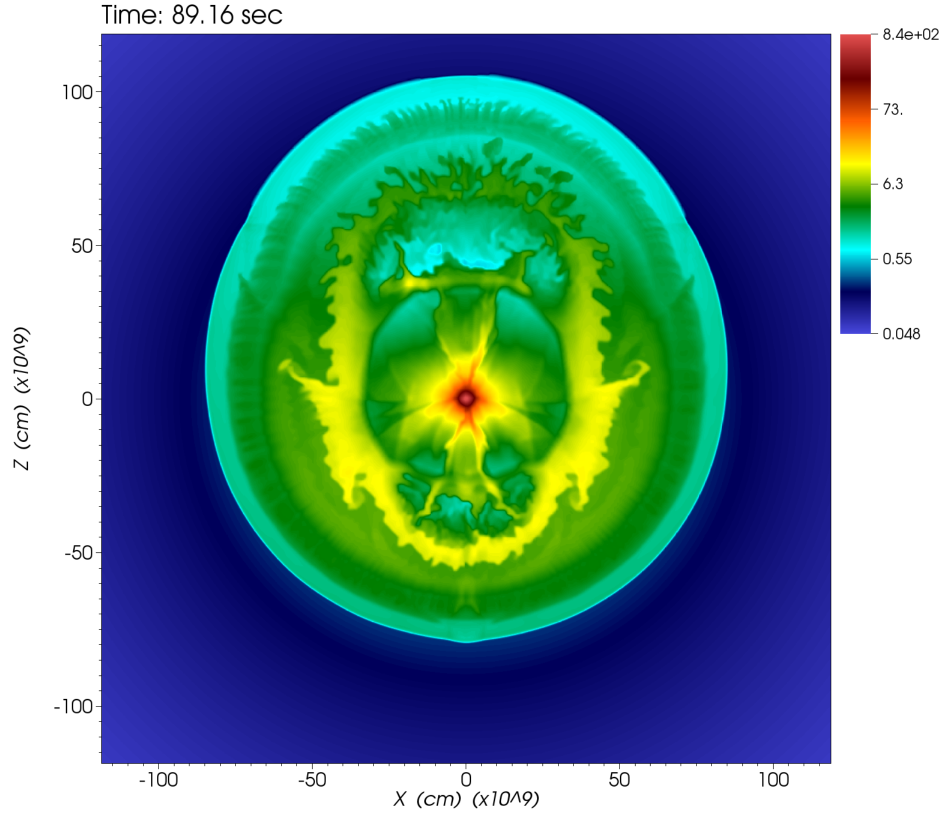

Single star

b18.3 vs n16.3: distribution of elements

MO et al. 2019a, in prep.

b18.3

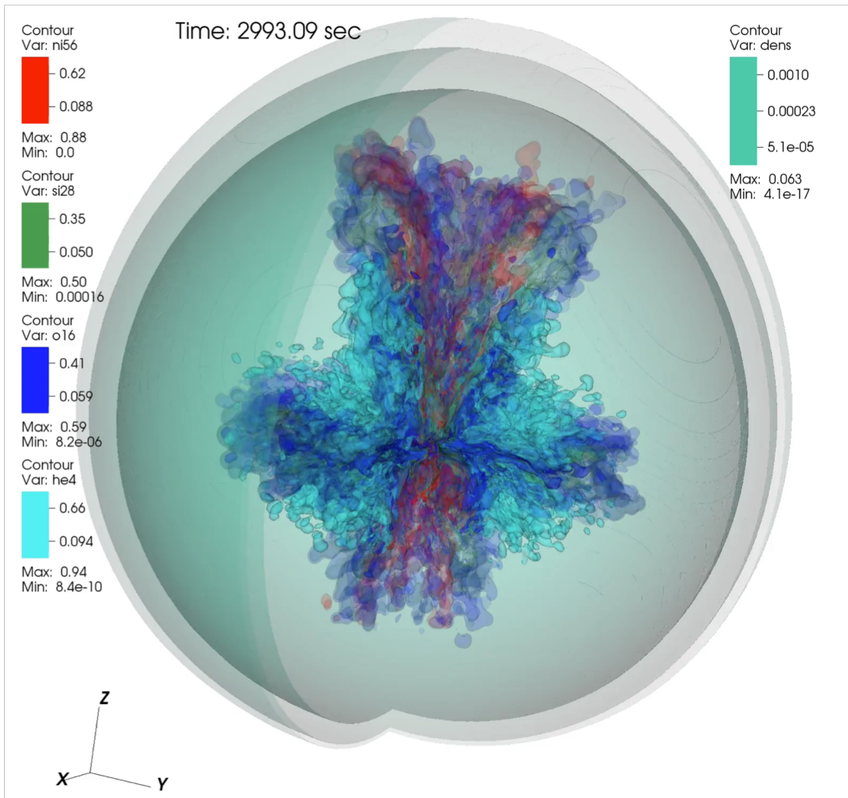

Binary merger

n16.3

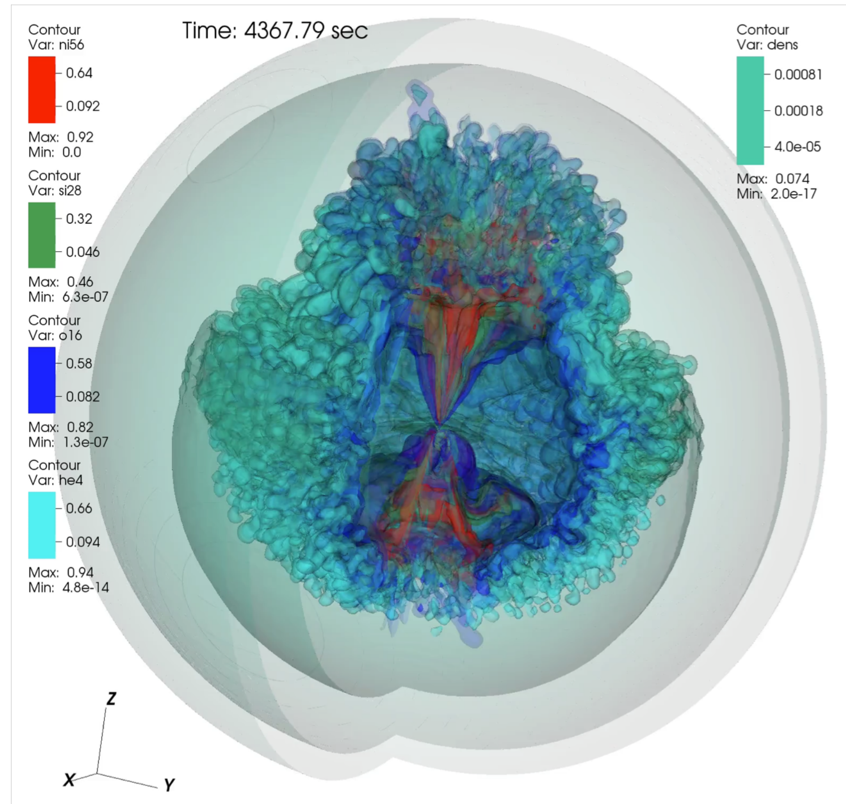

Single star

^{56}Ni (Red) ^{28}Si (Green) ^{16}O (Blue) ^{4}He (Sky blue)

Line of sight velocity distributions of ^{56}Ni

MO et al. 2019a, in prep.

b18.3 (binary model)

n16.3 (single star model)

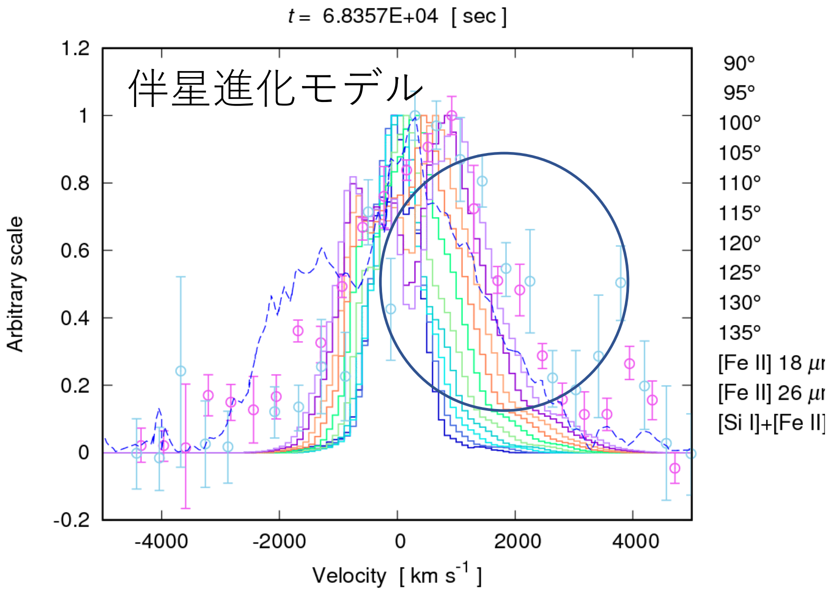

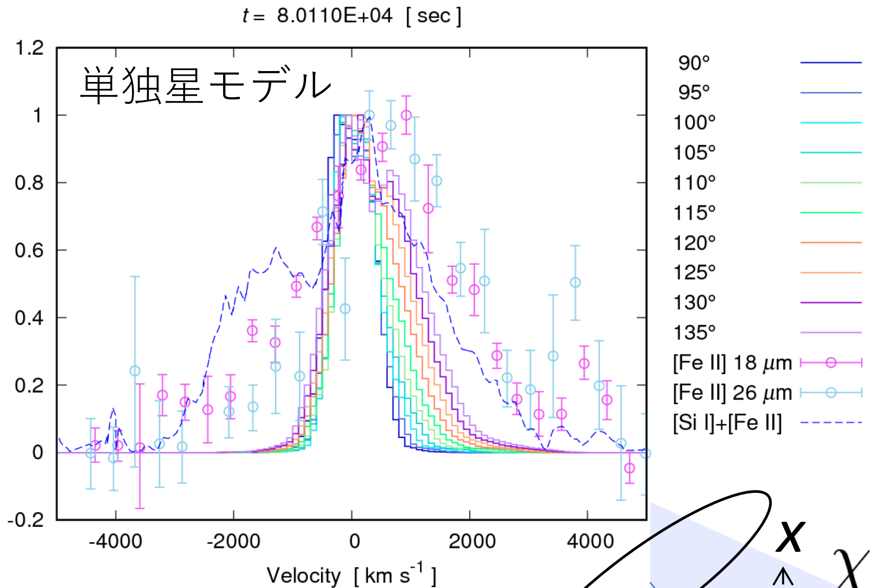

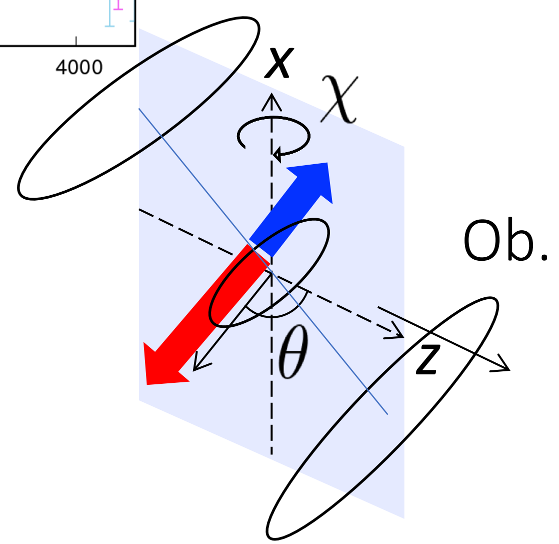

- The best model:
  - Progenitor model: b18.3 (binary merger model)
  - (E_{in}, α, β) = (2.5 x 10^{51} erg, 1.5, 16.0)
  - θ = 130°, χ = 10°

3D simulation of SNR phases

SNR evolution over 50 years

Orlando et al. 2019, in prep.

Basic methods are based on Orlando et al. 2015, ApJ, 810, 168

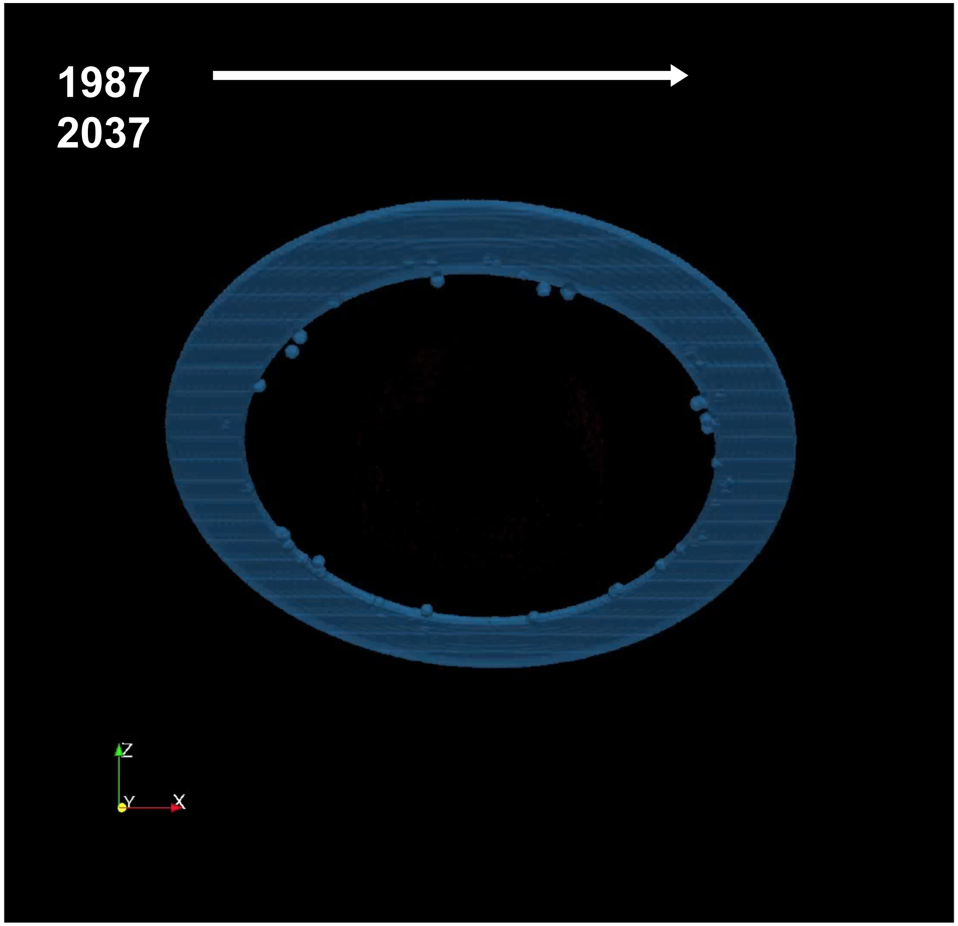

the physical model reproducing the observables of the supernova (the cause) is able to reproduce also the observables of the subsequent expanding remnant (the effect)

PLUTO
(Mignone+ 2007)

Abundances from Zhekov+ (2009)
ISM Absorption: 2.35e21 cm^{-2} (Park+ 2006)
Distance: 51.4 kpc (Panagia 1999)

Progenitor model dependence

Orlando et al. 2019, in prep.

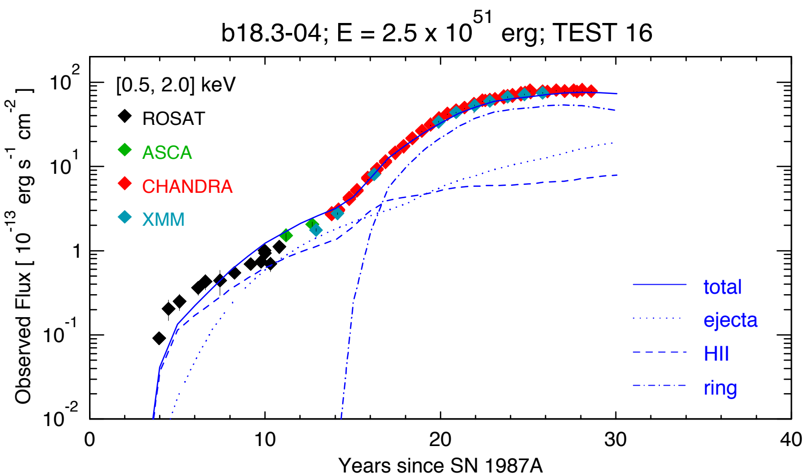

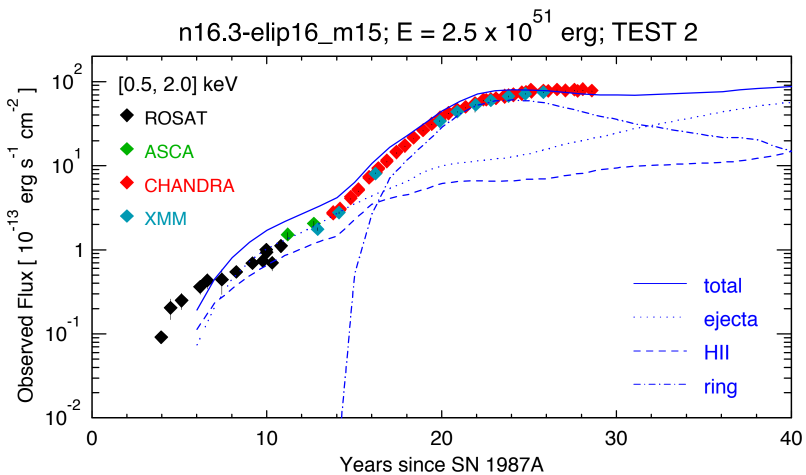

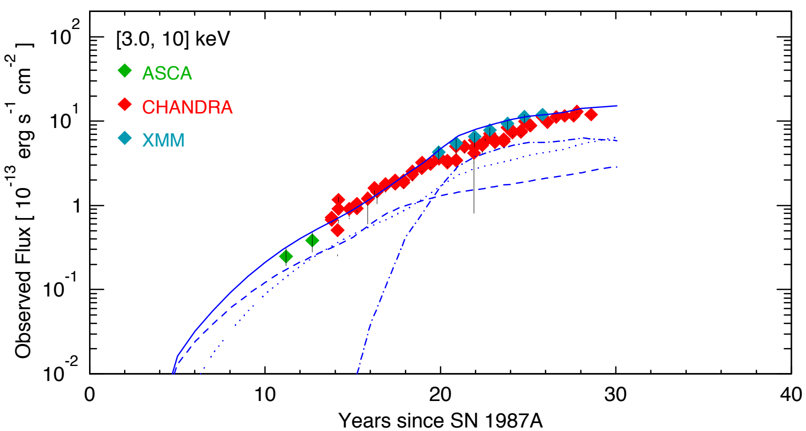

Binary merger model

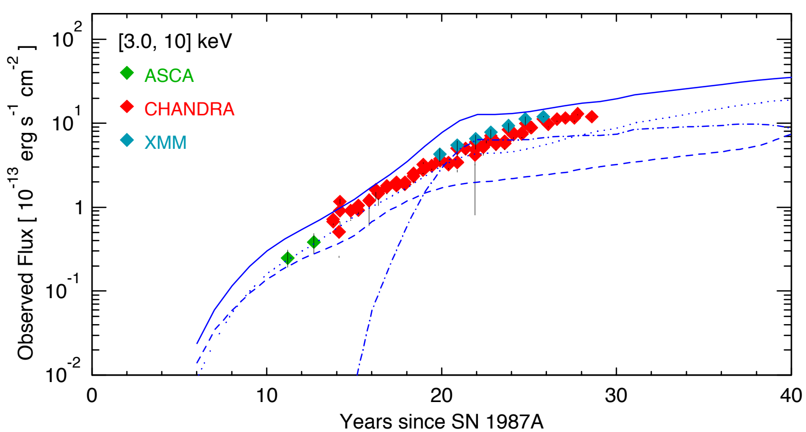

Single star model

The figure shows a 3D volume rendering of the density of the equatorial ring (ER) in 2015. The figure includes also the distribution of CO (red) and SiO (green)

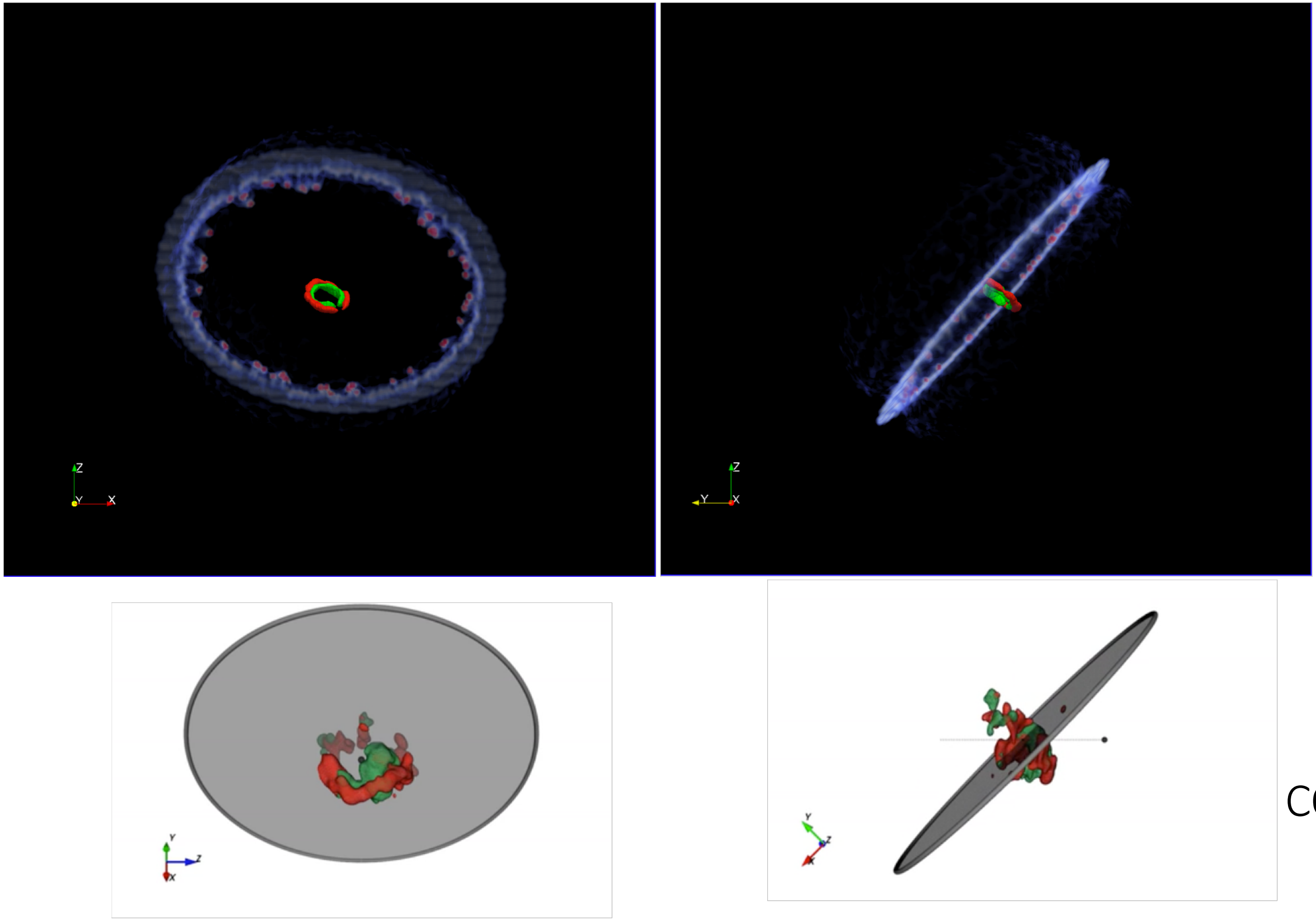

Orlando et al. 2019 in prep.

Abellan+ (2017)

Observation

CO distribution is ring-like ?

C x O, Si x O distribution (Top half) vs. Observation (Bottom half)

Molecule formation calculation

- Molecule network calculation is done based on the SN simulation results (1 day after the explosion) for each Eulerian grid

- Temperature and density evolutions 1 day after the explosion are assumed as power laws

$$\rho(t) = \rho_0 \left(\frac{t}{t_0}\right)^{-3} \qquad T(t) = T_0 \left(\frac{t}{t_0}\right)^{-3(\gamma-1)}$$

Density & temperature histories of test particles from 1D simulation : b18.3

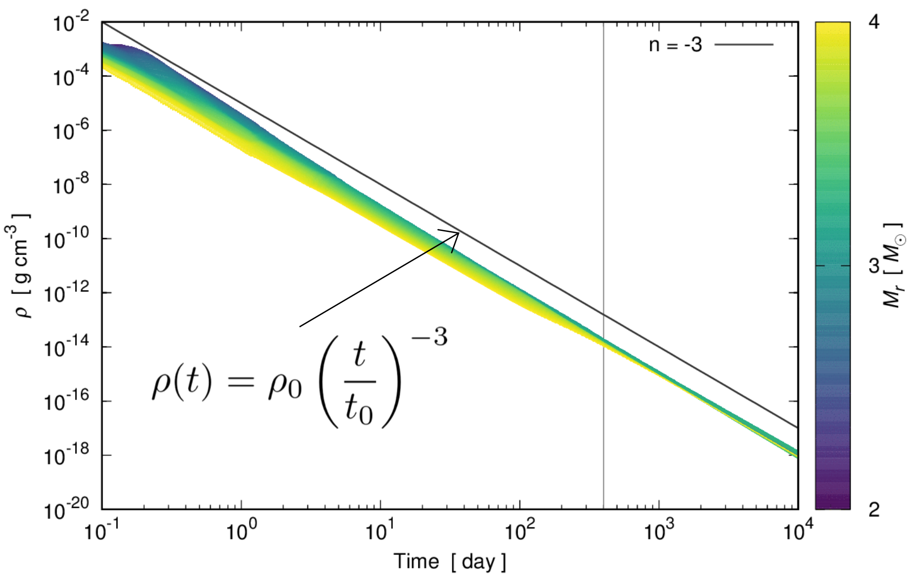

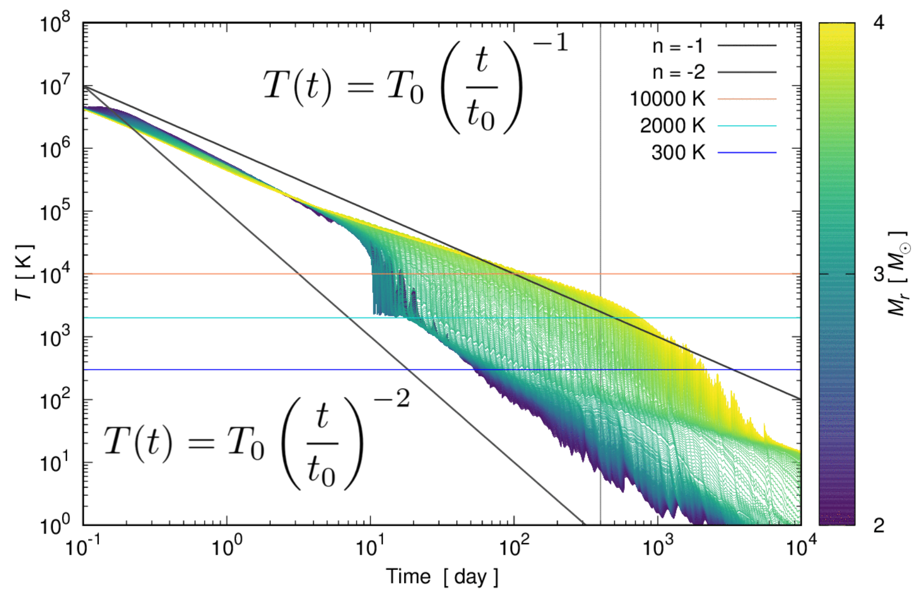

- Density seems to evolve as $\propto t^{-3}$
- Temperature seems to evolve as $\propto t^{-1}$ - t^{-2}

Molecule formation and destruction

Atoms: He, C, O, Ne, Mg, Si, S, Ar

Molecules: C_2, CO, O_2, SiC, SiO, CS, SO, Si_2, S_2

Formation rate coefficients

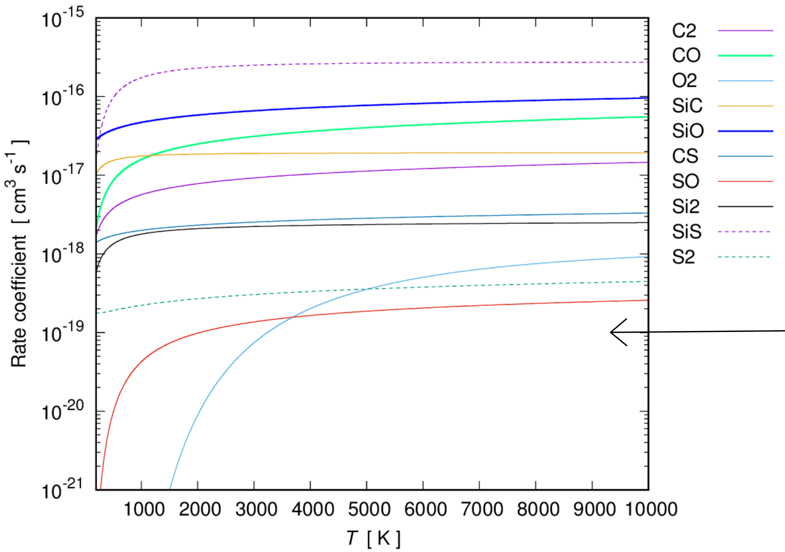

$$\frac{dc_i}{dt} = \underline{F_i} - \underline{D_i}$$

C_i: number density of i th molecules

Formation

$$k_i(T) c_k c_l$$

Destruction by the collision of particles

$$D_i(T) = c_i \sum_k \frac{1}{1+\delta_{ik}} c_k \, S_{ik} \, G_{ik}(T)$$

$$k_i(T) = A_i \left(\frac{T}{300 \text{ K}} \right)^{\alpha_i} \exp(-\beta_i / T) \quad [\text{cm}^3 \, \text{s}^{-1}]$$

$$S_{ik} = \pi (a_{0,i} + a_{0,k})^2$$

$$S_{ik} \, G_{ik}(T) = \langle \sigma v \rangle = \frac{4 \, S_{ik}}{(2\pi\mu)^{1/2} (k_B T)^{3/2}} \int_{E_{\mathrm{b},i}}^{\infty} E \exp\left(-\frac{E}{k_B T} \right) dE$$

$$= S_{ik} \left(\frac{8\pi k_B T}{\pi\mu} \right)^{1/2} \exp\left(-\frac{E_{\mathrm{b},i}}{k_B T} \right) \left(\frac{E_{\mathrm{b},i}}{k_B T} + 1 \right)$$

Coefficients for molecule formation

Molecular species (i)	Reactions	A_i [a] ($cm^3\ s^{-1}$)	α_i [a]	β_i [a] (K)
SiC	$C + Si \longrightarrow SiC + \gamma$	2.038×10^{-17}	-0.01263	136.73
C_2	$C + C \longrightarrow C_2 + \gamma$	4.360×10^{-18}	0.35	161.31
Si_2	$Si + Si \longrightarrow Si_2 + \gamma$	2.190×10^{-18}	0.045	258.79
SiS	$Si + S \longrightarrow SiS + \gamma$	4.175×10^{-16} [b]	-0.108[b]	741.54[b]
CS	$C + S \longrightarrow CS + \gamma$	1.529×10^{-18} [c]	0.22	0.0
CO	$C + O \longrightarrow CO + \gamma$	1.360×10^{-17}	0.41	340.0
SiO	$Si + O \longrightarrow SiO + \gamma$	3.235×10^{-17} [c]	0.31	0.0
S_2	$S + S \longrightarrow S_2 + \gamma$	1.374×10^{-19}	0.3339	-78.801
SO	$S + O \longrightarrow SO + \gamma$	1.114×10^{-19} [d]	0.2761[d]	1297.9[d]
O_2	$O + O \longrightarrow O_2 + \gamma$	8.346×10^{-23} [e]	3.4880[e]	4624.7[e]

Arrhenius form $$k_i(T) = A_i \left(\frac{T}{300\ \mathrm{K}}\right)^{\alpha_i} \exp(-\beta_i/T) \quad [\mathrm{cm^3\,s^{-1}}]$$

MO et al. 2019b, in prep.

Number density of CO & SiO: $\gamma = 5/3$

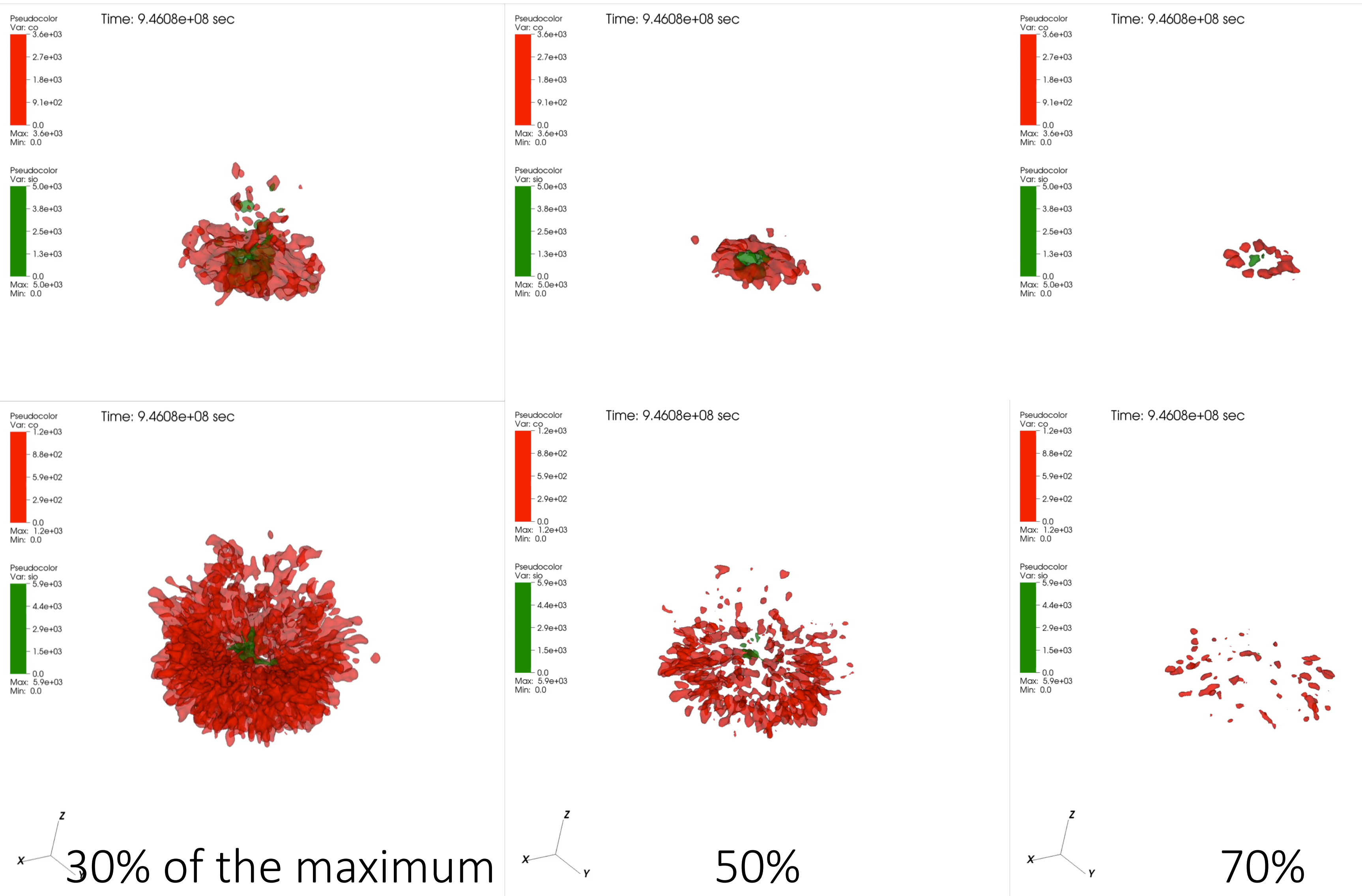

30% of the maximum | 50% | 70%

b18.3 (binary merger model)

n16.3 (single star model)

Calculated total masses of molecules

Assumed temperature evolution
γ: adiabatic index

$$T(t) = T_0 \left(\frac{t}{t_0} \right)^{-3(\gamma-1)}$$

Molecular species	b18.3 Total mass $[M_\odot]$			n16.3 Total mass $[M_\odot]$		
	$\gamma = 1.25$	$\gamma = 1.50$	$\gamma = 1.67$	$\gamma = 1.25$	$\gamma = 1.50$	$\gamma = 1.67$
C_2	3.38×10^{-4}	2.20×10^{-3}	4.07×10^{-3}	1.12×10^{-4}	2.40×10^{-3}	5.23×10^{-3}
CO	3.45×10^{-2}	2.80×10^{-1}	2.85×10^{-1}	4.49×10^{-2}	1.91×10^{-1}	1.96×10^{-1}
O_2	2.26×10^{-5}	3.25×10^{-4}	9.47×10^{-4}	2.73×10^{-4}	1.40×10^{-2}	3.74×10^{-2}
SiC	5.72×10^{-4}	1.15×10^{-3}	2.44×10^{-3}	4.87×10^{-5}	4.43×10^{-5}	8.91×10^{-5}
SiO	3.52×10^{-2}	2.85×10^{-1}	2.92×10^{-1}	3.46×10^{-2}	1.11×10^{-1}	1.12×10^{-1}
CS	7.17×10^{-5}	1.84×10^{-4}	1.32×10^{-4}	3.58×10^{-6}	4.70×10^{-6}	3.79×10^{-6}
SO	6.68×10^{-6}	7.72×10^{-4}	3.30×10^{-3}	4.64×10^{-6}	7.77×10^{-4}	2.71×10^{-3}
Si_2	1.81×10^{-5}	8.98×10^{-6}	4.81×10^{-5}	3.86×10^{-6}	6.95×10^{-6}	3.08×10^{-5}
SiS	7.67×10^{-3}	2.12×10^{-2}	1.11×10^{-2}	3.15×10^{-3}	7.01×10^{-3}	5.84×10^{-3}
S_2	5.85×10^{-7}	2.43×10^{-4}	1.33×10^{-3}	4.55×10^{-7}	1.06×10^{-4}	4.69×10^{-4}

- SiC molecules are produced much in b18.3 model with the aid of mixing
- Observations (Matsuura+17), 1.0 - 0.02 $M_\odot$ of CO and $2\text{x}10^{-3}$ – 4 x 10^{-5} $M_\odot$ of SiO, suggest majority of SiO has gone to dust ?

親星モデルの違いが物質混合、元素分布、分子形成に影響する

Summary and future work

- 3D hydrodynamical/MHD simulation of SN 1987A from the explosion to an early phase of the supernova remnant
    - Outcomes sensitively depend on the density structure of the progenitor models
    - Line emissions, such as [Fe II] could be a good indicator to estimate the explosion morphology
- Molecule formation calculation
    - Distribution of CO and SiO looks like the recent observation of 3D distribution (perpendicular to ER)

Future work

- Molecule formation calculation based on realistic density and temperature histories
- Dust formation/destruction calculation